A.C. CALORIMETRY OF DMPC LIPOSOMES

By

STEVEN GAYLE BLACK

Bachelor of Science

Emporia State University

Emporia, Kansas

1976

Submitted to the Faculty of the Graduate College
of the Oklahoma State University
in partial fulfillment of the requirements
for the Degree of
DOCTOR OF PHILOSOPHY
July, 1982

A.C. CALORIMETRY OF DMPC LIPOSOMES

Thesis Approved:

George S. Dixon / Gerald Pierce
Thesis Adviser

Jack J. Martin

Bruce J. Anderson

V. C. Pandit

Norman N. Durham
Dean of the Graduate College

ACKNOWLEDGMENTS

The author wishes to express his deep appreciation to his major adviser, Dr. George S. Dixon, for his assistance, patient guidance, and encouragement throughout the course of this research.

Appreciation is extended to the other committee members, Dr. H. J. Harmon, Dr. B. J. Ackerson, and Dr. M. G. Rockley for their assistance. Additional thanks is also expressed to Dr. J. J. Martin and Dr. N. Purdie for serving as substitutes on the committee.

The Physics-Chemistry Machine Shop was instrumental in the construction of the experimental apparatus. Appreciation is expressed to Heinz Hall for much advice and patience. A note of thanks is extended to Ms. Janet Sallee for her excellent typing of the manuscript.

Appreciation is extended to N.S.F. for funding without which this research could not have been done.

Finally, the author expresses special gratitude to his wife, Joyce, for her understanding and encouragement throughout the course of his graduate studies.

TABLE OF CONTENTS

LIST OF FIGURES

CHAPTER I

INTRODUCTION

The existence of cells has been known since Hooke observed the structure of cork in 1665. All living matter is composed of cells, a fact first concluded correctly by Dutrochet in 1824. The separate sections of the cell were observed in following years, but the study of the functions of the cell parts was not seriously undertaken until after 1907. This became possible when Harrison discovered a technique to grow isolated animal cells in vitro.

The cell is a separate entity in the case of bacteria and a semi-separate one for higher forms of life. With this realization the importance of the cell membrane became obvious in that, as stated by A. Szent-Gyorgyi (1):

> The cell membrane divides the universe into two parts, the 'inside' and the 'outside'. By this the cell membrane becomes the most important organ of the cell for it is here where the two worlds, the inside and the outside, meet (p. 211).

Much is known about the cell membrane, but yet much remains to be learned. This experiment was designed to study cooperative structural transformations in one of the components of cell membranes: the phospholipid bilayer which forms the matrix in which the active components of the membrane are imbedded. The particular system studied was multilamellar aqueous suspensions of synthetic dimysterolphosphatidylcholine (DMPC). DMPC, a phospholipid, is one of many types that are found in cell membranes. The technique used, known as differential a.c.

calorimetry, was first developed for use with crystalline samples and just recently applied to fluid samples. The differential form of this method was developed in this laboratory.

The cell membrane, more properly called the plasma membrane, is only one of the several membranes existing in the cell. Each of the membranes within the cell define semi-separate entities known as organelles. Each of the organelles has a composition which is different than the world outside the cell. In order for each organelle and the cell as a whole to function, mechanisms must exist to transport materials selectively through the membranes. In addition, membranes have many other different specialized functions. These include lipid synthesis, protein synthesis, and energy conversion (1).

The plasma membrane is composed of mostly lipids and proteins of varying types, and with some membranes having a small amount of cholesterol present (2). The discussion will now focus on the following: 1) What is the structural orientation of the membrane? 2) What mechanism forces the membrane to orient in the way it does? 3) How are the functional duties of the membrane performed? 4) What is the phase behavior of synthetic lipid membranes in comparison to plasma membranes? and 5) How does the phase behavior effect the various transport properties of a lipid membrane, and transport and enzymatic activities of a membrane?

The structural orientation as shown in Figure 1 is the one now most commonly accepted and is known as the fluid mosaic model (1). The model can explain the transport properties, the highly variable ratio of lipid to protein, and the various enzymatic activities of different types of membranes in at least a qualitative way (1). The model works particularly

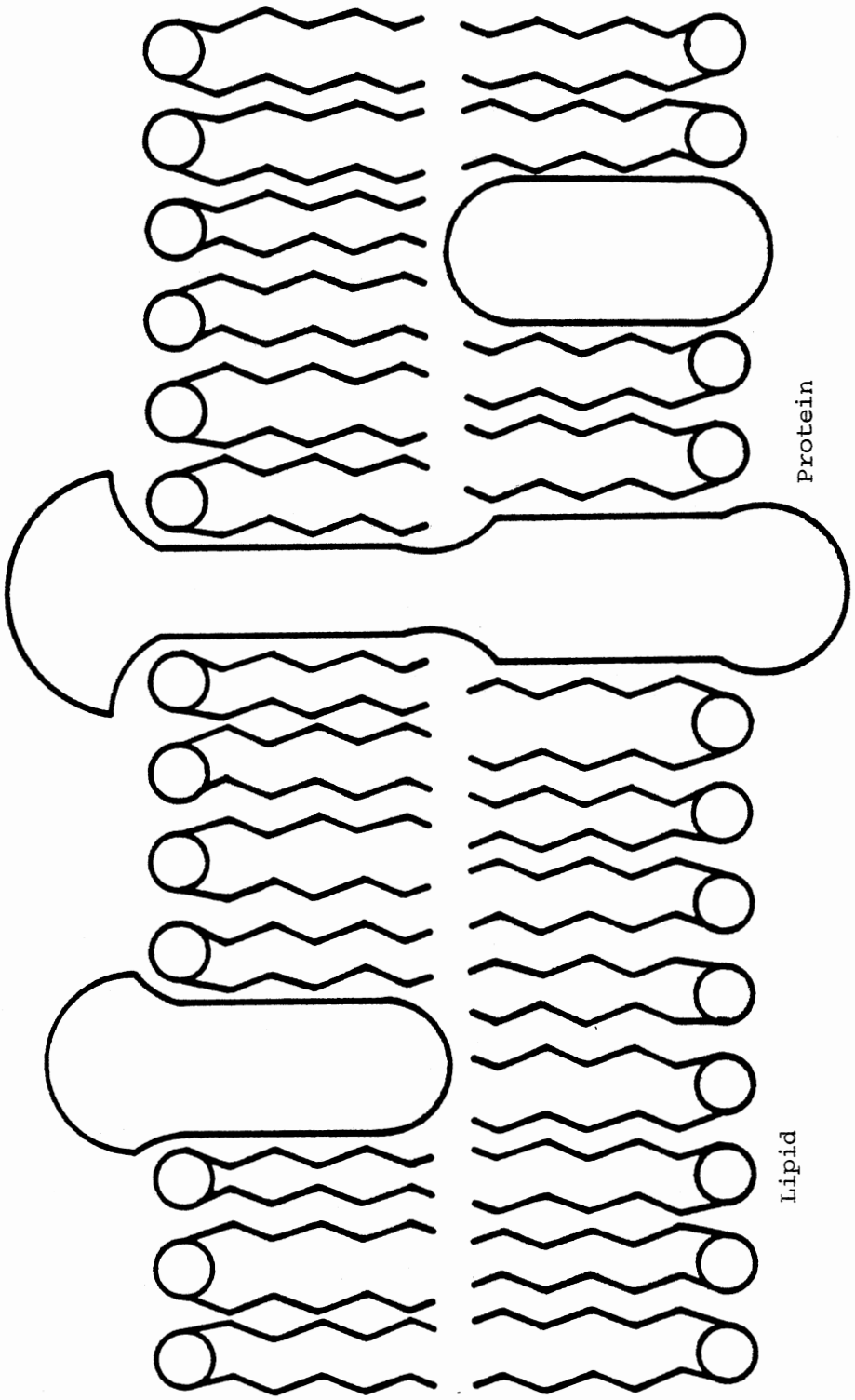

Figure 1. Fluid Mosaic Model of a Membrane

well in describing plasma membranes. But like many models it should not be considered an absolute one.

The lipids which comprise the backbone of the membrane consist of a hydrophobic portion and a hydrophilic portion. The hydrophilic portion of the molecules are, at the least, polar in nature and in some instances carry a net charge. This portion then can associate and interact with water, a polar molecule. The hydrophobic portion, consisting of hydrocarbon chains, is highly non-polar and therefore tends to not interact with water to the extent that the chains much prefer interacting with each other. This attraction is called a hydrophobic bond, which is not a bond in the chemical sense, but a way of saying they prefer each other's presence rather than the presence of water (1). This lipid bilayer serves as a highly efficient barrier for most substances (3). The diffusion rate (0.0001 - 1.0 mole/cm^2/hr/mole per ℓ) through a lipid bilayer is 10^6 to 10^9 times smaller than the free diffusion rate (2). The diffusion rate depends on the size of the molecule, its lipid solubility, and the lipid composition.

There are three general types of protein placement in the membrane. Some proteins in the bilayer extend completely through the bilayer, others only project through one side or the other, while others are just closely associated with the membrane surfaces. Each of the different placements of the proteins serves a different physiological purpose (1). The placement of the protein is, like the lipid arrangement, controlled by hydrophobic requirements. Proteins are large molecules having some portions hydrophobic and others hydrophilic. For example, the protein extending totally through the bilayer has a large hydrophobic center section with small hydrophilic sections on each end.

The proteins extending through the exterior face are often carbo-

hydrate-containing proteins. This type of protein is known as a glycoprotein (1). The glycoproteins act as binding sites to attach cells together to form tissue. The receptor sites for hormones are often glycoproteins. The receptor site is activated by the presence of the hormone and its interaction with another outer-surface protein. The transmission of the hormone's message is completed when the interacting exterior face proteins interact with an interior face protein or proteins (1). Those proteins that extend completely through the membrane act as a means of transport for materials needed inside the cell. Transport is probably accomplished by conformational changes in the responsible protein (1). The transport rate is regulated, in some cases, by other molecules, such as calcium. This transport may either be active transport or facilitated diffusion. The former requires the expenditure of energy, the latter does not. The difference lies in whether or not the transport is energetically favorable.

Because most intercellular proteins carry a net charge, the cell can accumulate a concentration gradient of ions across the membrane. Thus water, which passes rather easily through the membrane, rushes in to reduce the concentration gradient. If this were allowed to continue, the cell would develop sufficient internal pressure to burst. There is a membrane protein that exists to regulate the internal pressure of the cell. This protein, named the sodium pump, must exist because sodium has an energy-of-entry level that is highly favorable (1).

Active transport, facilitated diffusion, and the sodium pump all move molecules or ions across the plasma membrane. In many cases, this requires proteins to interact with each other and in some cases may require the protein to change conformation. Thus, the ability of the proteins to operate depends on their ability to move within the membrane.

Fluidity or the absence of fluidity depends for the most part on the thermodynamic state of the hydrocarbon chain portion of the membrane lipids. Calorimetric studies of lipid vesicle suspensions which contain only one type of lipid find a sharp, narrow phase transition which occurs at a particular temperature (6-8). This phase transition occurs when the hydrocarbon chains melt or become disordered. The temperature at which this happens depends on the length and degree of saturation of the hydrocarbon chains in the particular lipid, and the type of headgroup.

The fluidity of a membrane is also affected by the amount of cholesterol present. Cholesterol is more often found in animal cells than in plant or bacterial cells. Calorimetric studies have determined that the addition of small amounts of cholesterol to a lipid membrane lowers the main phase transition temperature slightly and decreases the enthalpy of transition (4,5). The addition of more cholesterol increases the effect until at cholesterol concentrations of 33 mole % the transition totally disappears. Cholesterol's effect seems to be to isolate the lipid molecules from each other because cholesterol is a nonpolar molecule and inserts into the bilayer in the lipid hydrocarbon tail region. This allows the hydrocarbon tails to continually change conformation and a phase transition of the lipids is not seen.

As cell membranes contain many different types of lipids, studies have been done to determine the melting behavior of mixtures of different lipids (5,9). There have been two basic types of results obtained, for a mixture of two different lipids. First, if the transition temperatures of the two types of lipids are sufficiently separated, two distinct phase transitions are observed. Each transition resembles the phase transition observed for that particular lipid. If the two transition

temperatures are sufficiently close together, the transitions tend to overlap. The phase transition appears basically as one wider, less distinct transition with decreased enthalpy. As more types of lipids are added to the system the transition broadened further and became even less distinct. In studies performed on cell membranes it is this behavior that was seen (5,10). The phase transition often was many degrees wide with the onset of the transition poorly defined while the termination was more distinct.

This type of transition behavior is known as phase separation. When the temperature is increased from a value just below the phase transition; the process starts first with the lower temperature melting lipids doing so while those that melt at higher temperatures still have not melted. As the temperature is raised more of the lipids melt. So at temperatures partially through the broad transition there are areas of melted lipid and areas of unmelted lipid, thus the term phase separation.

Studies performed on cell membranes both with and without the membrane proteins intact have shown that the transition behavior is approximately the same (5,10). Two peaks were obtained in the data when intact membranes were used. One peak was said to result from the phase transition of the lipid component and the other from denaturation of the protein. This was shown to be true in two ways. Subsequent rescanning of the same sample exhibited no protein denaturation peak as would be expected. Secondly, data obtained on membranes with the protein extracted showed only the peak associated with the phase transition of the lipid component. Thus the lipid-protein interaction is not extensive in respect to the chain melting, and the fluidity of the membrane is largely controlled by the types of lipids present. In this respect synthetic

lipid bilayer vesicles are a good model for studying the lipid component of cell membranes.

Calorimetric studies have been found to be beneficial in determining the structure of lipid membranes, particularly by studying the phase behavior. Since the fluidity of the membrane changes dramatically upon passing through the main phase transition, the question arises as to the relevancy of the phase transition. Does a living cell function only at temperatures greater than or less than the phase transition, or does it function best at temperatures within the transition? One such way to determine this is to measure the growth rate of cells at different temperatures. Experimental work on bacteria has found that the bacteria grow at temperatures within the phase transition (4,5,10). The growth rate did not reduce significantly until the temperature was reduced to a point that was about half way through the transition. As the temperature was reduced further the growth rate fell rapidly. At the temperature in which only about 10% of the membrane was fluid growth ceased entirely.

Many cells, such as M. laidlawii bacteria, have the ability to incorporate lipids composed from the fatty acid media in which they are grown. These bacteria then have the ability to change their transition temperature greatly. Studies performed on M. laidlawii found that the transition temperature was a function of growth conditions (4,5,10). The temperature at which the bacteria were grown was found to lie within the phase transition.

For growth to occur, newly synthesized lipids and proteins need to be inserted into the cell membrane. Thus it appears that for the insertion to occur the membrane has to be in the fluid state or at least localized portions of sufficiently large size have to be in the fluid

state. When the fluid regions are small enough or isolated enough, insertion, and thus growth, is no longer possible.

So it appears that there is no physiological reason for the membranes of cells to change phase. In fact at temperatures below the phase transition growth ceases to occur. But many cells grow within the phase transition and when given the opportunity to adjust their phase transition do so but just enough to remain within the phase transition. Thus it is probably not necessary for the cell to exist in the entirely fluid state and in many cases temperatures above the transition are detrimental to cell growth (10). So there must be some physiological reason for being in the partially fluid state.

Many studies have determined the permeability of lipid membranes as a function of temperature (11-15). The glucose permeability of DMPC vesicles increased dramatically between 20 ^{o}C and 23 ^{o}C (18). This is close to the transition temperature of 24 ^{o}C. The addition of 25 mole % egg lecithin into the vesicles decreased the enhanced diffusion at temperatures above the transition. The addition of small amounts of cholesterol, less than 30 mole %, to the DMPC vesicles increased the enhanced diffusion above the transition. But for amounts of cholesterol above 30 mole %, the enhanced diffusion was decreased. At amounts of 40 mole % cholesterol, transport showed little temperature dependence. Diffusion of $^{22}Na^{+}$ through dipalmitoylphosphatidylcholine (DPPC) vesicles was shown to peak at DPPC's transition temperature of 42 ^{o}C (14). The diffusion rate above the transition was larger than the rate below the transition. K^{+} diffusion was shown to peak at a value of 25 ^{o}C, near the transition temperature, for DMPC vesicles, and the diffusion rate of similar ions depended on their size (15). As the ion's diameter increased

the diffusion rate decreased. Not only did the diffusion rate depend on the size of the ion, but the diffusion rate also depended on the hydrocarbon chain length. As the chain length increased the peak diffusion at or near the transition temperature decreased (11). Cl^- ions were found to diffuse faster through egg phophatidylcholine vesicles than K^+ ions (11). Valinomycin increased both K^+ and Cl^- diffusion in DPPC vesicles (12).

The results of studies on phospholipid vesicles show enhanced diffusion rates at the transition temperature. But biological membranes are much more complex and perform many functions other than acting as a semipermeable membrane. Measurements of the rates of proline uptake and enzymatic (succinic dehydrogenase) activity on E. Coli found that discontinuities exist for the functions at temperatures which depend on the lipid incorporated into the membrane (16). But the temperatures at which these discontinuities occur is neither at the transition temperature of the intact membrane or of the lipids extracted from the membrane. Other results for E. Coli show rate discontinuities for respiration and ^{14}C efflux at temperatures which depend on the lipid incorporated into the membrane (17). The temperatures at which these rate discontinuities occurred were not well correlated with the thermal transition of the membrane. Molecular-motion data from spin-labeled mitochondria have shown a perturbation in the spin-label-motion parameter at certain temperatures (18). The temperatures at which the perturbation occurred was dependent on the species from which the mitochondria was isolated. This perturbation was thought to show a phase transition of the mitochondria, and at the same temperature the rate of oxygen consumption changed.

While evidence from biological membranes may or may not show trans-

port and enzymatic activity changes at the transition temperature of the membrane, many of the activities do show a temperature dependence. This temperature dependence does change when different types of lipids are incorporated into the membrane. This indicates that the enzymatic and transport activities depend on the thermodynamic state of the membrane. So cells living at a temperature where the transport and enzymatic activities are rapidly varying could adjust these activities with small changes in fluidity.

The thermodynamic state of the cell membrane has been found to be an important factor in the cell's function. Cells have been shown to grow well at a temperature within the phase transition. Evidence indicates that the cell functions best when at least part of the membrane is in a fluid state. The explanation for this seems to be related to the protein's ability to move laterally in the membrane, and the ability of ions to diffuse through the membrane. These functions are dependent on the fluidity of the membrane. The fluidity of the membrane is largely controlled by the type of lipid. Thus the understanding of the lipid component of the membrane is very necessary.

This study was undertaken for just this purpose. The experiment compared the profile of the heat capacity peak observed on heating through the transition with the peak observed on cooling through the transition for DMPC vesicles. This profile comparison was done as a function of annealing temperature. The results were used to attempt to characterize the molecular organization of the lipid bilayer. Thus with this better understanding of the molecular organization, the fluidity characteristics can be better understood. This can lead to a better understanding of the various transport and enzymatic activities of cell membranes.

CHAPTER II

PROPERTIES OF THE PHOSPHATIDYLCHOLINES

Molecular Structure

A molecule of biological origin which has a hydrophobic tail or tails, a lipophilic (soluble in nonpolar solvents) and hydrophilic head group has been classified as a lipid. The specific lipid used in this study is dimyristoylphosphatidylcholine (DMPC). As seen in Figure 2, a DMPC molecule consists of a phosphate linked-group, a glycerol type framework, a phosphate polar group and two hydrocarbon chains (3). The phosphate group, glycerol framework and phosphate linked group are often lumped together and called the head group. The hydrocarbon chains are known as tails. All phosphatidylcholines have the same basic structure, only differing in the length and degree of saturation (the number of double bonds) of the tails. DMPC has two identical myristic (14 carbon) acid chains with no double bonds.

When DMPC, as well as other phosphatidylcholines, is added to water, the molecules spontaneously orient themselves so as to isolate the tail region from the water. The structure formed is called a vesicle. This vesicle may be made of several bilayers which is known as a multilamellar vesicle or liposome as shown in Figure 3. If these multilamellar vesicles are sonicated for a sufficient period of time the structure formed is a vesicle consisting of one bilayer. These vesicles are known as uni-

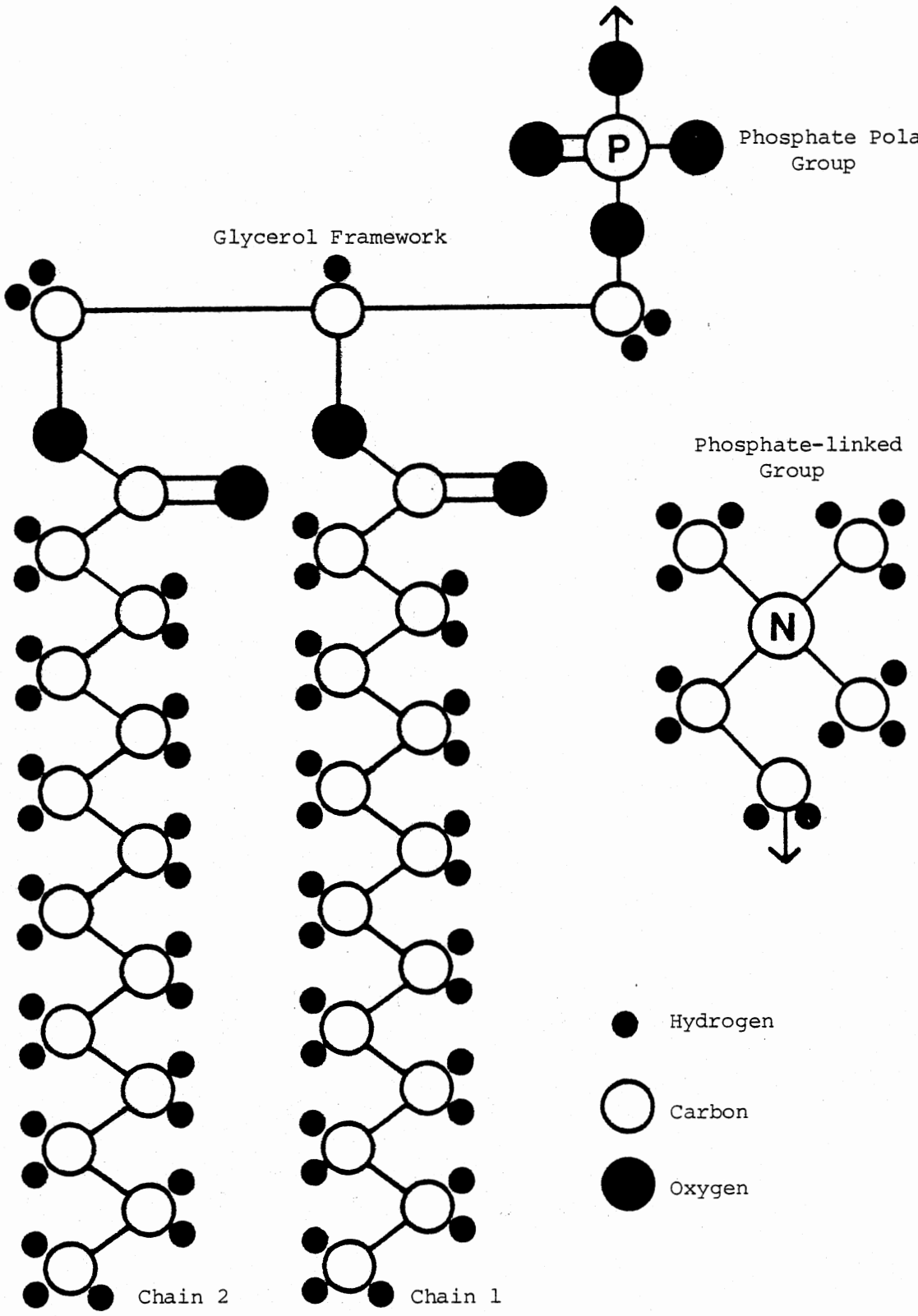

Figure 2. Molecular Structure of DMPC

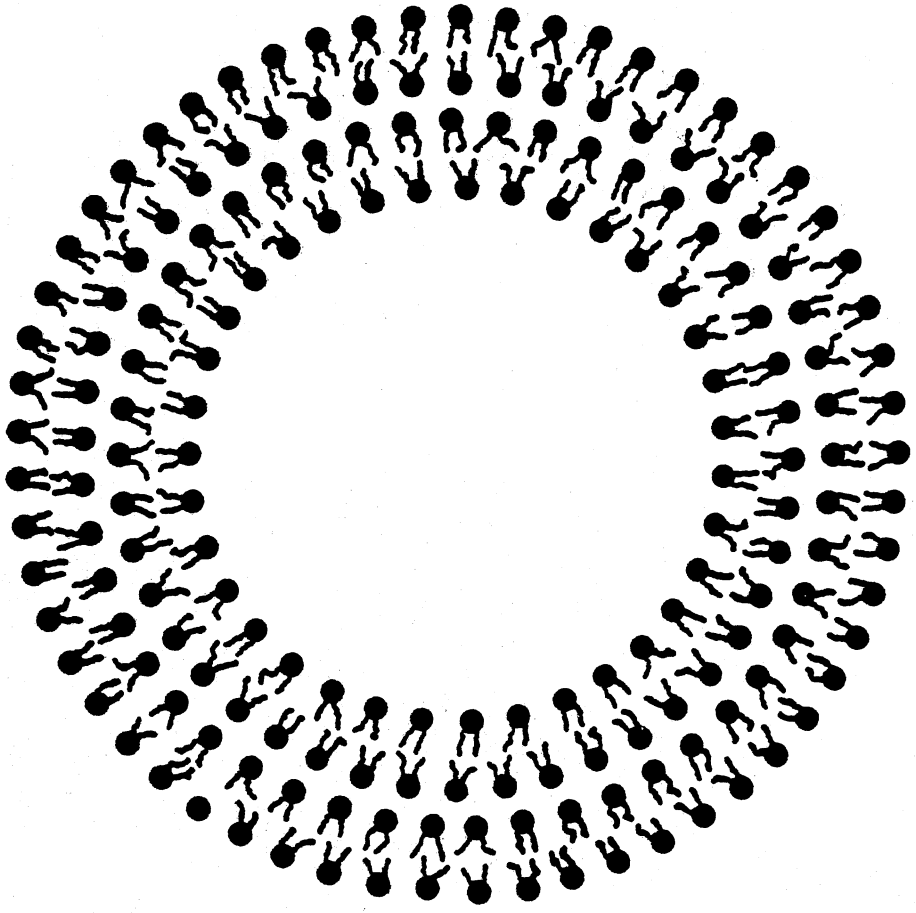

Figure 3. Phosphatidylcholine Liposome

lamellar vesicles. There are also other techniques used in forming various sizes of unilamellar vesicles (19,20).

Bilayer Structure

The bilayer structure or phase, which depends on the specific orientation of the phosphatidylcholine molecules within the bilayer, is found to be dependent on the temperature and the degree of hydration. This phase dependence has been extensively studied by the method of x-ray diffraction (21-26). One such phase diagram is shown in Figure 4 (26).

The notation used to distinguish between phases is now standard and describes the bilayer structure observed in a particular phase (21). An L phase is one in which the bilayer has a one dimensional (lamellar) lattice. A P type phase is one in which a two dimensional lattice exists, and C is the crystalline or three dimensional phase. The α and β' subscripts describe the orientation of the hydrocarbon chains relative to the bilayer plane. Type α is a liquid-like conformation of the chains. The chains are highly disordered, but the average chain orientation is perpendicular to the bilayer plane. The β' chains are stiff and fully elongated and lie at an angle tilted away from the perpendicular to the bilayer plane.

The L phase exists at water concentrations of less than 25% by weight and at temperatures less than $0^{\circ}C$. At temperatures greater than $0^{\circ}C$ and 25% water the DMPC is in the $L_{\beta'}$ phase. The x-ray experimental data show there is very little structural difference between the L and $L_{\beta'}$ phases (26). Calorimetrically, a transition has been observed between the L and $L_{\beta'}$ phase in DMPC (26) and DPPC (27,28). This tran-

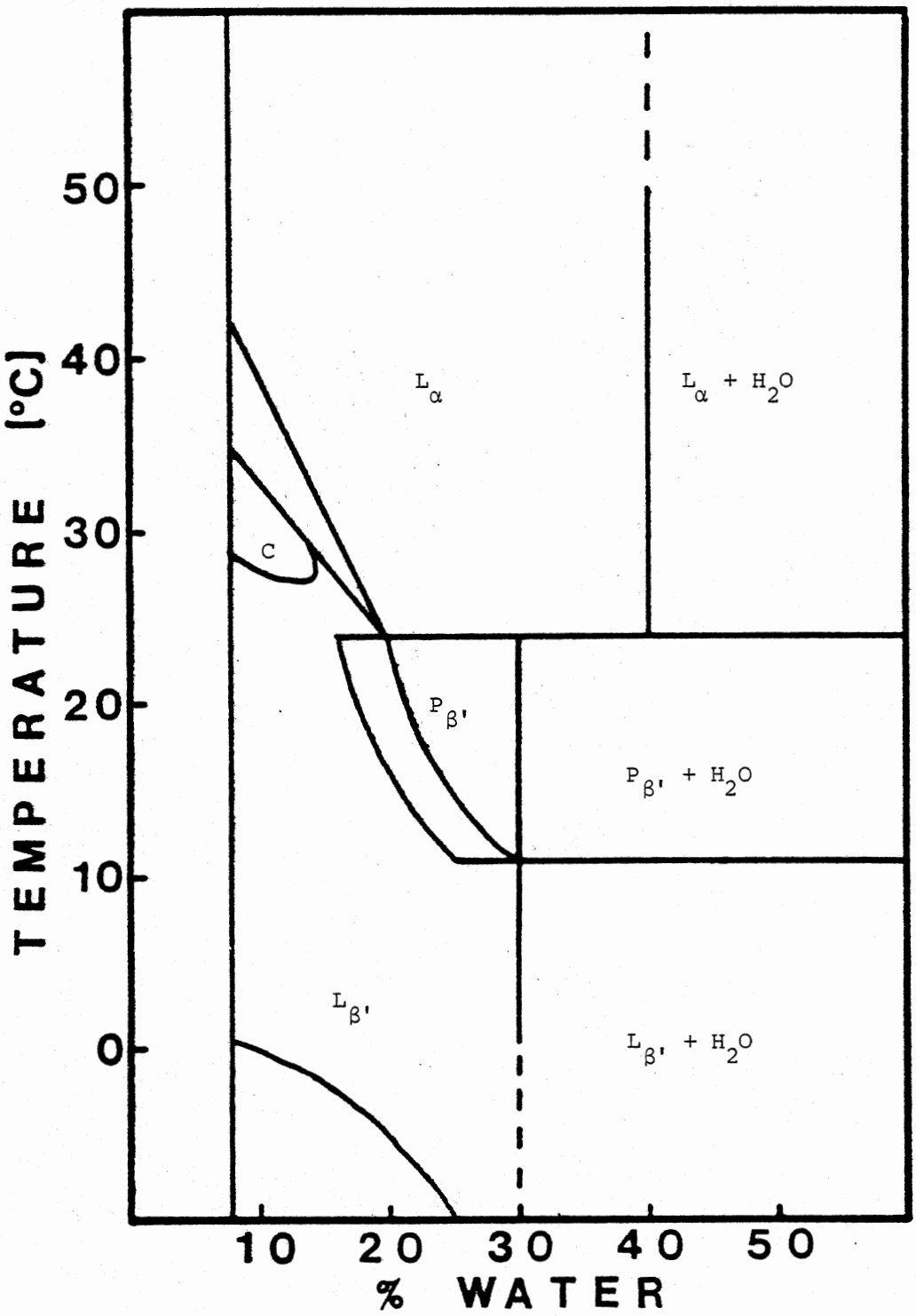

Figure 4. Phase Diagram of DMPC as a Function of Temperature and Water Concentration

sition could result from chain packing changes or from rearrangement of the interstitial water at the headgroup.

The $L_{\beta'}$ phase is a one dimensional phase with tilted, extended chains as shown in Figure 5 (24,26). The $L_{\beta'}$ phase exists at all water concentrations shown in the phase diagram for various values of temperature. At concentrations of water above 30% by weight the hydration requirement of the head groups has been satisfied and excess free water exists. The hydrocarbon chains are crystalline-like and tilted with respect to the bilayer perpendicular. The tilt angle decreases with increasing temperature. The hydrocarbon chains are packed in a 'distorted' hexagonal array with the interlamellar repeat distance, d, increasing from 53.6 Å at 18% water to a maximum value of 61.7 Å at 29% water. This lattice becomes less distorted as the temperature is increased. The bilayer thickness, d_t, is a function of hydration and decreases as the water content increases from the value of 47.1 Å at 10% water to a minimum value of 42.4 Å at 25% water. The value of d_t would be 51.6 Å if the chains were rigidly extended and perpendicular to the bilayer plane. So the values of d_t in the $L_{\beta'}$ phase are consistent with tilted chains. The average tilt angle is found to be 55 degrees with respect to the bilayer perpendicular for water concentrations greater than 20% at a temperature of 10 °C.

The pretransition is associated with the transition from the $L_{\beta'}$ to the $P_{\beta'}$ structure. The $P_{\beta'}$ structure is a two dimensional structure as shown in Figure 6 (22,26). The second dimension results from the periodic ripple in the lattice. The hydrocarbon chains are packed in a hexagonal array. The cell parameters (a,b) change little with temperature, but vary greatly as a function of a water content. The parameter, a,

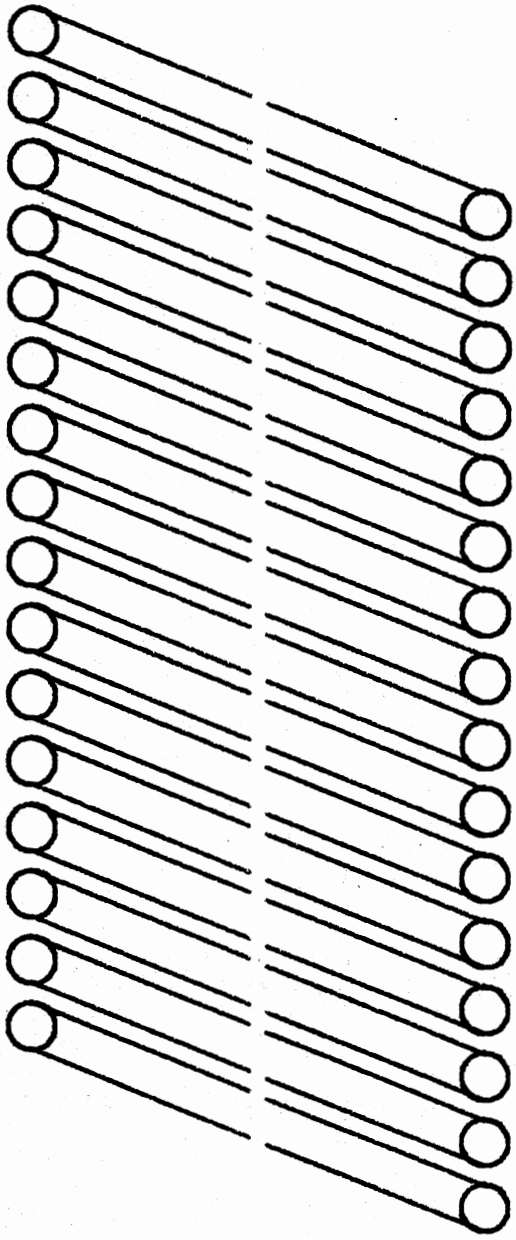

Figure 5. $L_{\beta'}$ Phase of DMPC

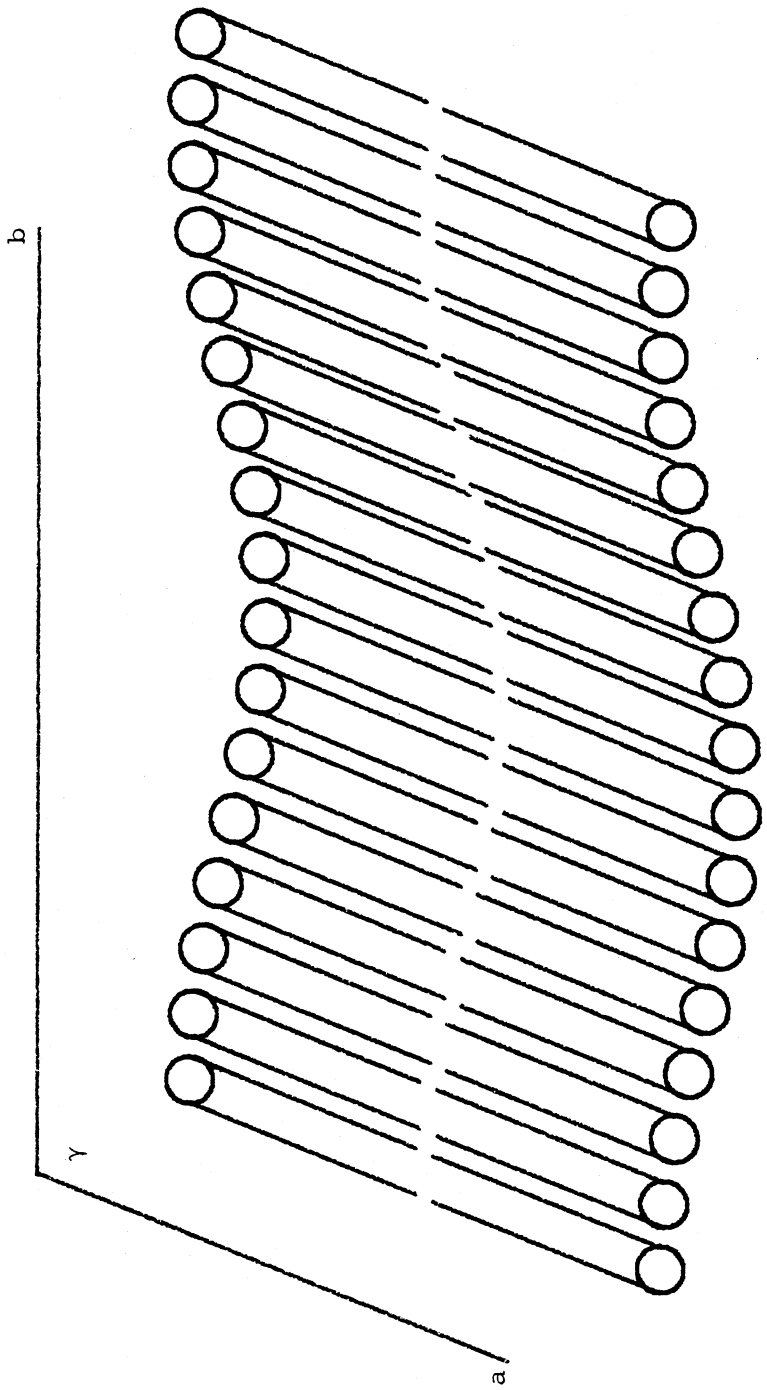

Figure 6. $P_{\beta'}$ Phase of DMPC

increases from a value of 57 Å at 21% water to a maximum value of 64.9 Å at 29% water, while the b parameter decreases from a value of 156 Å at 21% water to a minimum value of 120 Å at 29% water. Model calculations show the depth of the ripple to be about 15 Å (26). The hydrocarbon chains are rigid and tilted with respect to the bilayer perpendicular. Raman spectroscopic studies have shown that chain 1 is more nearly all trans (extended) than chain 2 (29). The tilt angle decreases with increasing temperature. NMR studies have shown that for DPPC (fully hydrated) in the $P_{\beta'}$ phase the molecules are rapidly rotating at high speed and the speed of this rotation decreases with decreasing temperature (30). This result is most likely true for DMPC fully-hydrated bilayers also.

Within a small range in temperature (27 - 35 °C) and water concentration (9 - 14%) a crystalline (three dimensional) phase exists. The cell is orthorhombic with indices, a = 53.8 Å, b = 9.33 Å, and c = 8.82 Å (22). This phase may coexist with other phases. At low water concentrations a two phase region exists, which contains the L_{α} phase along with either the C, $L_{\beta'}$, or $P_{\beta'}$ phases depending on the water concentration.

The main phase transition is associated with the transition from the $P_{\beta'}$ to the L_{α} structure. The L_{α} phase, as shown in Figure 7, exists at a temperature greater than the chain melting temperature for all water compositions (24,26). The interlamellar repeat distance, d, starts to increase at 21% water. This corresponds to the water concentrations at which free water is present. At this same point the bilayer thickness, d_t, starts to increase from its minimum value of 35.5 Å to a maximum value of 62.2 Å. Structural perturbations are finished when the

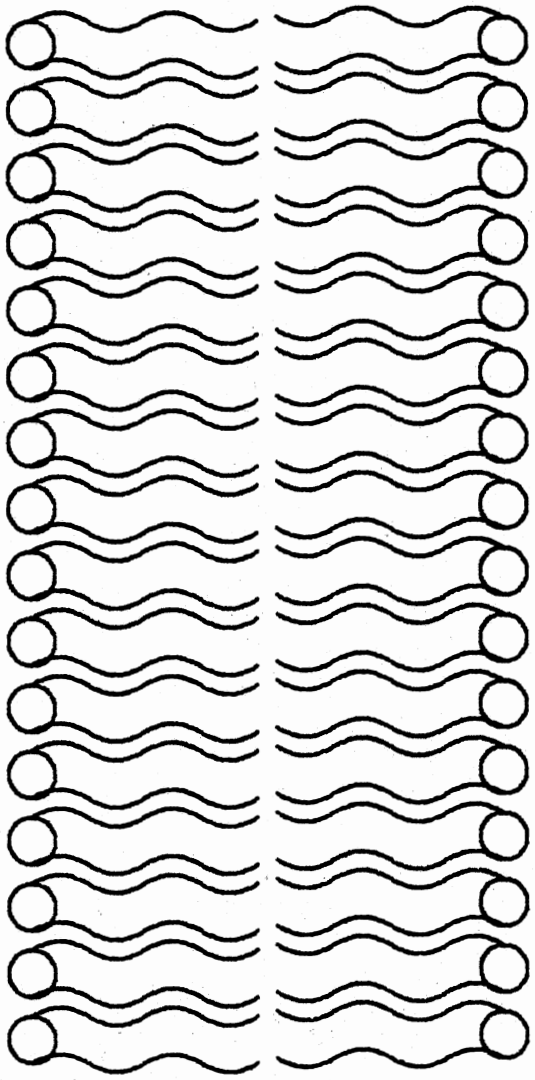

Figure 7. L_α Phase of DMPC

bilayer is hydrated to the point where free interstitial water is found between bilayers. The L_α phase is a one dimensional phase with the chains no longer stiff and extended. The chains become fluid-like with their orientation, on the average, being perpendicular to the bilayer plane. Deuterium magnetic resonance studies have shown that the two hydrocarbon chains in the lipid molecule are not physically equivalent (31-33). The beginning of chain 2 is essentially parallel to the bilayer plane. The disordering of the chains increases towards their ends.

NMR studies have shown that mixed phases exist when cooling a DPPC fully hydrated sample through the phase transition from the L_α to the $P_{\beta'}$ phase (30). This mixed phase existed for periods of at least 30 minutes. This seems to apply also to DMPC suspensions as shown by this study.

NMR studies have been done to characterize the orientation of the head group as a function of temperature (34). This study determined that for DPPC bilayers, which are fully hydrated, the orientation of the PO_4 portion of the head group was such that the O-P-O plane is inclined at an angle of 47 ± 5 degrees with respect to the bilayer normal. The O's are the nonesterified ones of the PO_4 group. This tilt angle is not a function of temperature and, therefore, would seem to indicate that the head group contributes little to a phase transition. The study was done on DPPC but DMPC is identical to DPPC except for their chain lengths. Thus one would expect approximately the same tilt angle for DMPC bilayers in excess water. There are two possible orientations for the remainder of the head group, $N(CH_3)^{3+}$. The first is that this group folds back on itself and bonds to the PO_4. This is not likely because this conformation appears sterically unfavorable. The second possibility is that the

$N(CH_3)^{3+}$ extends approximately parallel to the bilayer plane.

Calorimetric Observations

The pre- and main-phase transitions of fully hydrated DMPC have been extensively studied by conventional differential scanning calorimetry for heating scans (7,8,9). Figure 8 shows a typical result. The pre-transition, or $L_{\beta'}$ phase to $P_{\beta'}$ phase transition, has been found to have an enthalpy change of 1.0 kcal/mole at a transition temperature of approximately 14 ^{o}C. The half width of this transition is greater than 1^{o}C. The main transition, or $P_{\beta'}$ phase to the L_{α} phase transition, has an enthalpy change of 5.0 to 5.4 kcal/mole. This transition occurs at a temperature of 23.9 ^{o}C with a half-width as small as 0.15 ^{o}C for highly pure samples.

Transition Models

Experimental studies have determined that the hydrocarbon chains of phosphatidylcholines undergo a disordering process during the thermally induced transition from the $P_{\beta'}$ phase to the L_{α} phase. Many models have been proposed to theoretically describe the chain melting process. In general a model must consider the various interactions and conformations that the bilayer undergoes. Some of these requirements that must be considered are: 1) conformation of the hydrocarbon chains, 2) dimensionality of the transition, 3) comparison of the bilayer transition with known hydrocarbon melting and other intermolecular features, 4) the role of water, 5) intermolecular interactions, 6) Van der Waals interactions, 7) interactions between head groups, and 8) interactions between the two monolayers of a bilayer (35).

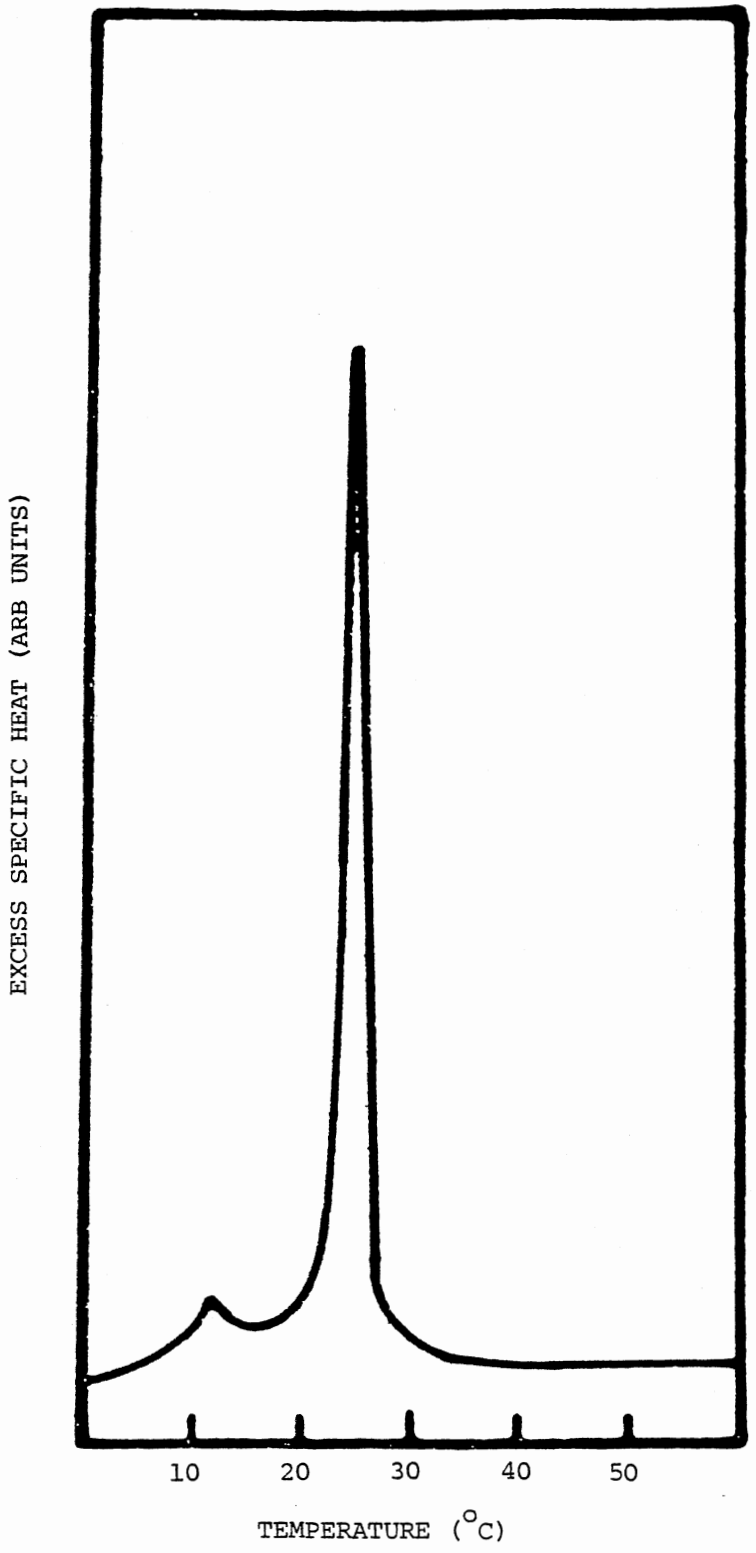

Figure 8. Typical Heat Capacity Curve for DMPC as Measured by Differential Scanning Calorimetry

The conformation of the hydrocarbon chains is as seen by experiment the most important degree of freedom. In principle this would require that a model allow for continuous changes of the angle, θ_i, between neighboring carbon-carbon bonds. But models have shown that it is sufficient to use only three states for each bond, the ordered state ($\theta_i = 0^\circ$) and a doubly degenerate disordered state ($\theta_i = 120^\circ$).

Because of interest in dimensionalities of less than three, it was hoped that the bilayer would exhibit a two dimensional type phase transition. Two dimensional modeling worked reasonably well except near the phase transition temperature. Thus a practical model has to be a three dimensional one.

The main phase transition involves the disordering of the hydrocarbon chains. Since the melting process of alkanes is well understood, one might think that the disordering of the hydrocarbon chains is similar to the melting of alkanes. But the disordering of the bilayer produces a change in entropy and volume that is only about half that of the alkane of same chain length. This result is a consequence of a hydrocarbon chain in a lipid molecule being constrained by its attachment to the head group. An anisotropy is introduced, and the amount of disordering is reduced in comparison to an alkane. In addition the two hydrocarbon chains are not physically equivalent.

Water plays a very important role in that the lipid does not exist in the bilayer form without its presence. The bilayer remains intact both above and below the phase transition. The hydrophobic interaction is only slightly changed by the phase transition. Water separates the bilayers in a liposome, but a single bilayer and a liposome have the same transition temperature. Thus the interaction between bilayers

need not be considered. Only the small changes in head group interactions with water, that occur during the phase transition, need be considered for a fully hydrated liposome.

The intermolecular interactions are very important in that without these interactions the transition would not exist. At low temperatures the hydrocarbon chains are in the low energy extended configuration. If no intermolecular interactions existed the chains would disorient continuously on increasing temperature. With the bilayer packing arrangement that exists, the chains are not free to disorder gradually. The disordering must then occur cooperatively producing a phase transition.

Although the hydrophobic requirements are responsible for the bilayer formation and continued existence, other interactions are much more important afterwards. The excluded volume effect limits the minimum volume. The expansion of the bilayer is constrained by the hydrophobic effect and attractive Van der Waals interactions. At the transition temperature the Van der Waals interaction dominates. For DPPC the change in enthalpy of the transition is calculated to be approximately 5.5 kcal/mole for the Van der Waals part and 0.2 kcal/mole for the hydrophobic effect (35).

Interactions such as dipolar, excluded volume, hydrogen bonding between phosphate groups, and nonspecific Van der Waals forces exist between the carbonyl groups, glycerol linkages and phosphatidylcholine head groups. Different head groups can change the transition temperature by approximately 20 ^{o}C, but this is a smaller effect than unsaturating one carbon-carbon bond and comparable to adding two CH_2 groups to the chains of the lipid molecule. The repulsive head group interactions prevent the molecules with chains perpendicular to the bilayer plane

from coming close enough together to minimize the Van der Waals interactions between the hydrocarbon chains at temperatures below the transition. By tilting the molecules the head groups can remain separated, and the ordered chains can be close enough together to minimize the Van der Waals interaction.

In addition to the interactions among molecules in each side of the bilayer there exist interactions between each monolayer of the bilayer. An important thermodynamic parameter is the area per molecule. It has not, so far, been possible to impose a variable external surface pressure on a bilayer. This is easily done on monolayers. When the surface pressure on a monolayer is varied a phase transition occurs. But the behavior of monolayers and bilayers is quite different. Theoretically when one assumes a surface pressure of 50 dynes/cm for both the monolayer and bilayer the transition temperatures are approximately the same. This leads to a change in area per molecule and change in enthalpy of the transition that is much smaller in the monolayer case. For surface pressures of 20 dynes/cm, the area and enthalpy changes are the same for both the monolayer and bilayer, but the transition temperatures are different. Unlike bilayers, monolayers don't seem to exhibit a first order phase transition. Thus a bilayer cannot be strictly thought of as two back to back monolayers.

A model must include at least the Van der Waals attractive interactions between the chains and an excluded volume (repulsive) interaction for a phase transition to be exhibited. Proposed models have attempted to satisfy these requirements in several different general ways. These vary from adapting models developed to describe other systems to models attempting to describe the chain orientation in detail.

The simplest model exhibiting a phase transition is known as mean field theory (35). The model can include both important interaction terms, but in some cases the mean field interaction includes terms that have been added to produce agreement with experimental data (35). Some of these included terms have questionable theoretical basis. Identifying the terms in the Hamiltonian that correspond with real interactions is often difficult. Mean field theory is best for long range interactions and at its worst for short range ones such as excluded volume. Even though it has limitations the model has two strong points. The calculation is fairly easy to do,and the limitations of the model are well known. In some applications the statistics of each hydrocarbon chain can be calculated precisely.

Several techniques have been developed that treat the excluded volume effect in a better manner than mean field approximations. These calculations suspend a hydrocarbon chain or chains in a periodic potential and measure the chain configuration using a Monte Carlo technique. The first such attempt suspended three chains on a two dimensional hexagonal lattice (35). Unfortunately the attractive interactions were not included, and thus the model could not exhibit a phase transition. Later versions of this technique used a single chain, in a periodic three dimensional box, interacting with mirror images of itself (35). This method accounted for both the attractive and repulsive interactions with nearest neighbors, but by using mirror images the long range correlations between chains was overstated.

Further attempts were made to treat the excluded volume term in a more suitable and physically meaningful way. By modeling the molecule as a hard disc, both the attractive and repulsive interactions were

included. Although the model has not been exactly solved, calculations were performed using molecular dynamics. The interactions were determined as a function of molecular area and density. The molecular area is determined by the possible chain states. Various methods were used to parameterize the initial area states. One model had a fundamental difficulty in that the sum of the areas might not equal the area of the sum of two neighboring molecules (35). This could occur when the chains kinked and jogged, allowing them to interlace. This effectively softens the excluded volume interaction and makes the calculation much like that of mean field theory. Another model maintained the integrity of the excluded volume interaction, but simplified the chain statistics (35). All chain states giving the same area were grouped together and assigned a weight factor. In addition, the states were defined by using idealized chains on a square lattice.

In order to keep the modeling as simple as possible, two state models have been proposed (35). The chains are only allowed to be in two states, fluid or solid. This is just a spin one-half Ising model, of which much is known. The problem is that the chain statistics are greatly simplified and excluded volume interactions are excluded. The model is a reasonable approximation for only the Van der Waals attractive interactions.

All models that predict a phase transition exhibit varying degrees of success. The most successful models must treat the excluded volume repulsive forces and the Van der Waals attractive forces. This would include some mean field calculations, some chains suspended in a periodic potential calculations, with the best results obtained using the hard disc calculations. Mean field calculations often give enthalpy changes

that are too large. Although no calculation was made for chains of length greater than twelve, Marcejla's model produced transition temperatures that were too high (36). This result was obtained using no adjustable parameters other than the lateral pressure which was taken to be 20 dynes/cm. With their chain statistics model, Belle and Bothorel calculated the transition temperature of DPPC to be 36 ^{o}C (37). The actual transition temperature is 41 ^{o}C, and no other calculations were made. The hard disc calculation by Scott and Cheng is the most physically meaningful calculation and gave good results (38). The lateral pressure in the membrane was taken to be 50 dynes/cm and an adjustable parameter (the interaction strength) was fit so that transition temperatures matched those found experimentally. The enthalpy and change in attractive Van der Waals energies at the transition were found to agree well with the values found experimentally for DMPC, DPPC, distearoylphosphatidylcholine (DSPC), and dibehenoilphosphatidylcholine (DBPC).

CHAPTER III

EXPERIMENTAL PROCEDURE

Introduction

Calorimetry has an inherent advantage over other techniques often used in measuring phase transition behavior. These other techniques, such as spin resonance and fluorescence, require the insertion of molecular probes into the system. The molecular probes used in lipid bilayers position themselves in the hydrocarbon chain region and tend to alter the phase behavior and sample the local environment. Calorimetry does not require the insertion of a perturbing molecule and measures the bulk behavior of the sample.

Conventional differential scanning calorimetry, as the name implies, measures the heat capacity only when the temperature is changing. The sensitivity of the instrument increases as the temperature scan rate increases. The instrument is measuring the heat capacity, an equilibrium property, at scan rates as large as 30 ^{o}C/hr. This limits the temperature resolution of the phase transition and could possibly produce a distorted specific heat peak. In addition, most instruments are limited to increasing temperature scans.

The a.c. calorimetry technique originated by Sullivan and Seidel, has neither of the two problems exhibited by differential scanning calorimetry (39). The heat capacity is measured by the thermal response of the sample to small periodic heat pulses. This allows the heat

capacity to be measured during heating scans, cooling scans, and at constant mean temperature. Measuring the heat capacity at constant mean temperature allows one to determine if high scan rates distort the transition, if slow kinetic effects are occurring, and if the heat capacity varies as a function of time-varying conditions on the sample.

A.C. Calorimetry

The details of the a.c. calorimetry method have been discussed by others (39,40). An overview of the method will be presented, along with a solution to the problems encountered when applying the technique to a fluid sample at room temperature.

Consider a sample slab having infinite thermal conductivity, K, and heat capacity, C. The heat capacity includes that of the sample, sample container, heater, thermometer, and other addenda. The slab is constructed with an area that is large in comparison to its thickness as shown in Figure 9. With this simplification the problem becomes a one dimensional one. The slab is connected to a constant temperature (T_o = 0^oK) heat reservoir by a thermal resistance R on one face. The other face is heated by a sinusoidally varying heat flux $\dot{q}(o,t) = \dot{q}_o e^{i2\omega t}$, where $\dot{q}_o$ is the maximum value of the heat flux and 2ω is the angular frequency of the sinusoid. The relaxation times for the heater to slab and thermometer to slab are considered as negligible. That is the slab, heater, and thermometer all follow the same temperature as heat is applied. The temperature of the system is determined by the differential equation

$$C \frac{\partial T}{\partial t} = \dot{q} - T/R \qquad (1)$$

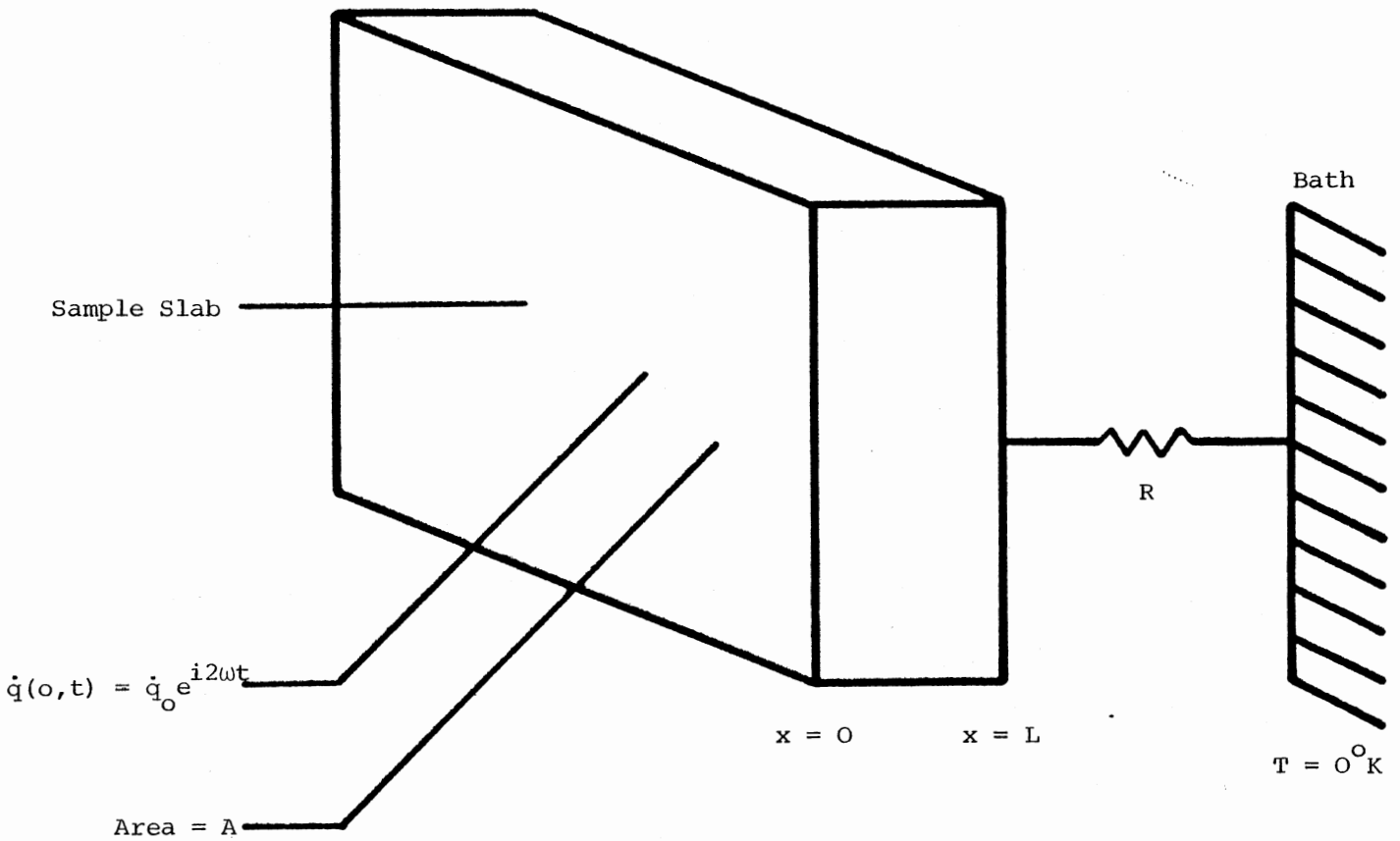

Figure 9. Slab-Shaped Sample of Thickness L Thermally Connected Through a Thermal Resistance R (to a Bath at x = L) and Having a Heat Input $\dot{q}(o,t)$ at x = O

This equation has a solution

$$T = T_{ac} e^{i2\omega t} \tag{2}$$

$$T_{ac} = \frac{-i\dot{q}_o}{2\omega C}\left(1 - \frac{i}{2\omega\tau_b}\right)^{-1} \tag{3}$$

with τ_b = RC defined to be the sample to bath relaxation time. If the requirement that $\omega\tau_b >> 1$ is imposed, the solution becomes

$$T_{ac} = -iq_o/(2\omega C) \tag{4}$$

which will be known as the ac temperature equation.

All real samples have a finite thermal conductivity. The solution can be calculated from the heat conduction equation. If the thickness of the sample is small in comparison to the characteristic length $\ell_o = (2\eta/\omega)^{\frac{1}{2}}$, where η is the thermal diffusivity, a similar solution is found. The small differences are due to heater-sample and sample-thermometer connections.

Thus arises the problem of applying the equation to a liquid sample at room temperature. The thermal diffusivity of the liquid, in particular water, is much smaller, typically one to two orders of magnitude, than the thermal diffusivity of a crystalline solid. As an example, the thermal diffusivity of water is 1.5×10^{-3} cm^2/s and the value for aluminum is 7.9×10^{-1} cm^2/s. Using these values, the characteristic length is then $\ell_o = (5 \times 10^{-2}/\omega^{\frac{1}{2}})$ cm for water and $\ell_o = (1.25/\omega^{\frac{1}{2}})$ cm for aluminum. If a frequency of 1 Hz is used, the characteristic lengths then become ℓ_o = 200 μm for water and 5 mm for aluminum. It is thus seen that the sample must be very thin or a very small heating frequency

must be used in order for the behavior of the system to be that described by the a.c. temperature equation. Very thin samples present a problem in that the sample container is difficult to construct, so that it neither leaks nor the thermal path length changes due to pressure changes and thermal expansion. This can easily occur when the cell is constructed with thin walls. Using a thick walled sample cell alleviates the leaking problem and the significant changes in thermal path length, but large addendum corrections must be made, as the sample cell then becomes rather massive, and the heat capacity of the cell becomes large in comparison to the heat capacity of the sample. Using a long period heat flux requires long data acquisition times. This is of some concern as biological samples can degrade with time.

To avoid the problems previously discussed, a differential a.c. calorimeter was developed. The sample is contained in a rigid, easy to seal aluminum cell in which the sample is contained in grooves each with a thickness less than the characteristic length. The limiting characteristic length is then that of the aluminum and not the sample. The sample cell can contain a larger volume of sample than one in which the sample is contained in one thin layer. The heat capacity of the addendum is removed by operating in the differential mode. With an identical reference cell the calorimeter can be operated at frequencies of a few hertz and thus keep the data acquisition time to a minimum.

When operating in the differential mode the sample cell has a heat capacity, C_c, of the cell and a heat capacity, C_s, of the sample. The reference cell has only the heat capacity of the cell, C_c. If the heat capacity of the cell, C_c, is much greater than that of the sample, C_s, then the differential temperature oscillation, T_{ac}, is found to be

$$T_{ac} \propto \frac{\dot{q}_o}{\omega} \frac{C_s}{C_c^2} \tag{5}$$

providing any phase difference between the two cells is negligible.

Calorimeter Design and Operation

The calorimeter design uses two identical sample cells. One cell contains the sample suspension, the other water. Each cell, as detailed in Figure 10, consists of an aluminum body with a rubber o-ring recessed into each end. The bottom cap, made of aluminum, has 7 concentric grooves in its upper surface. Each of these grooves is 300 μm wide and 250 μm deep giving a total sample volume of 7.7 μℓ. The total distance between the heater and the thermometer is 1 mm. This distance is sufficiently less than the characteristic length of aluminum for frequencies of 1 Hz or smaller. The top aluminum cap has a flat surface that makes contact with the bottom cap when the cell is assembled. Each cap is secured to the body with three symmetrically placed screws. The heater is a 100 Ω microchip resistor (Dale Electronics) attached to the top cap surface with epoxy. The leads on the heater chips are 30 gauge magnet wire. The a.c. temperature response detector is a microbead thermistor (Omega Engineering), having a nominal resistance of 5 kΩ at 25 ^{o}C, secured to the bottom cap surface with epoxy containing copper powder. The mean temperature of the cell is measured with a chromel-constantan thermocouple (Omega Engineering), attached to the bottom in a similar manner, referenced to an ice bath.

The sample and reference cells are mounted in a temperature regulated brass chamber, as shown in Figure 11. The temperature is regulated by circulating water from a thermostated bath (Haake Model FK-2)

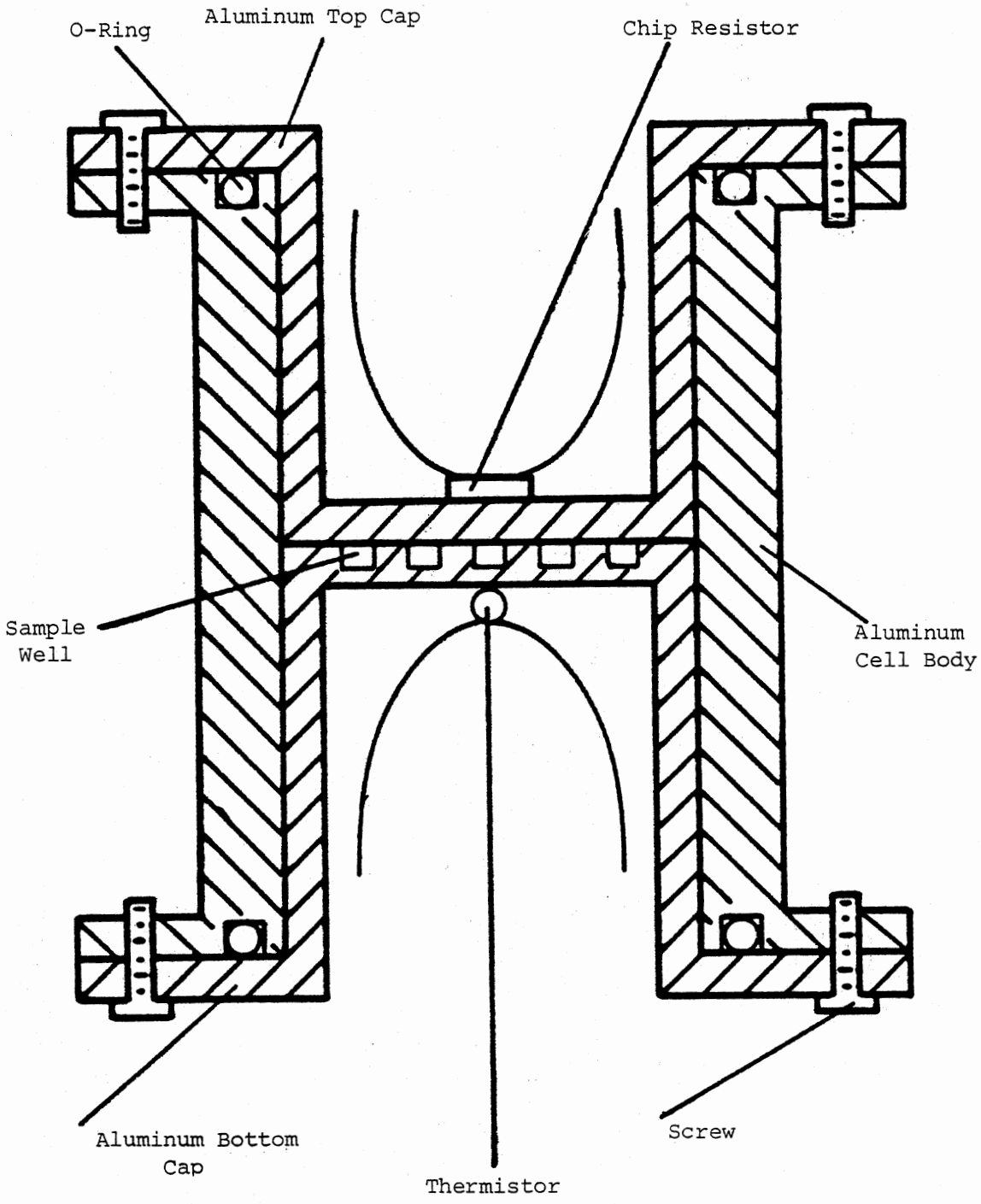

Figure 10. Sample Cell

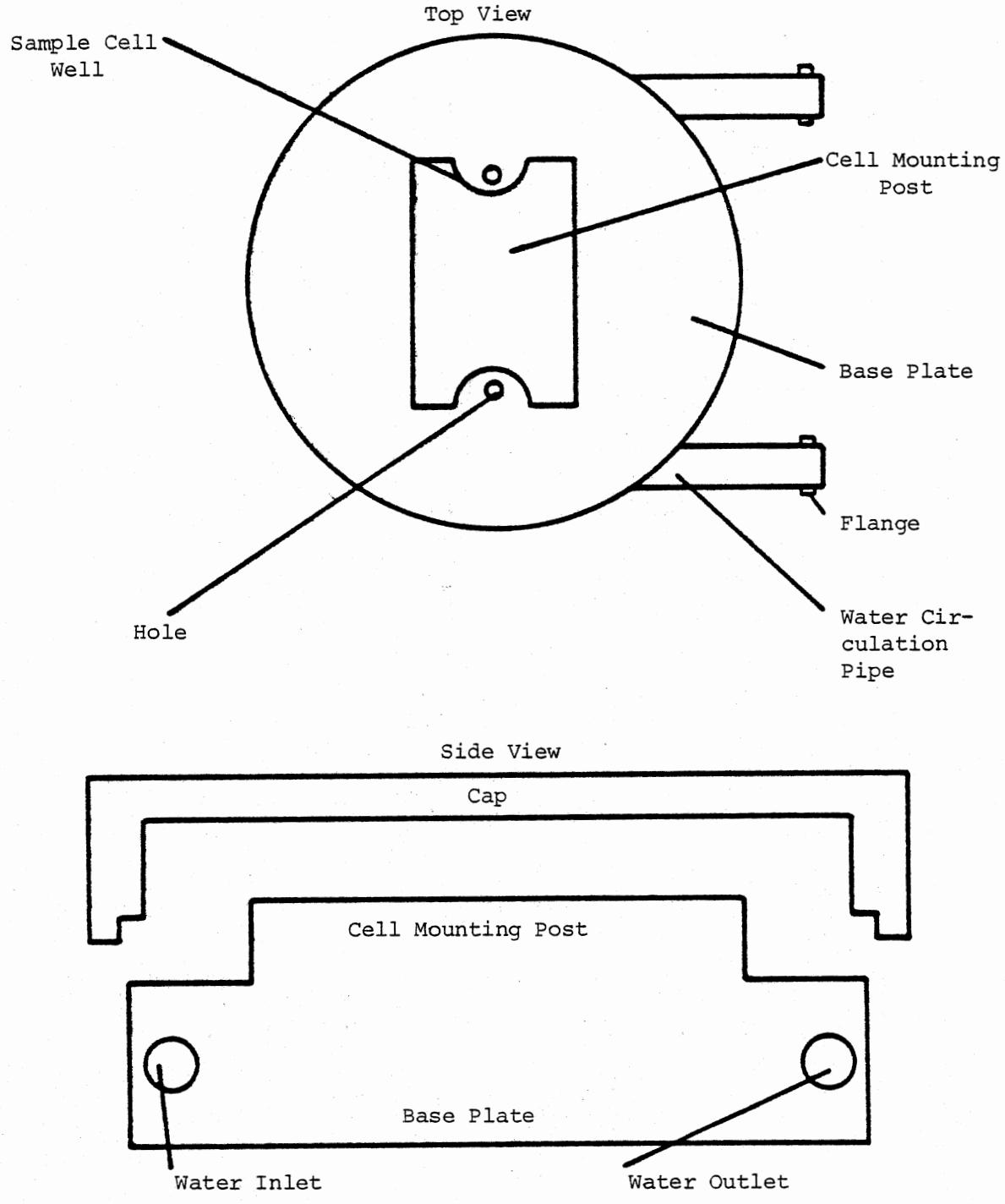

Figure 11. Brass Chamber

through the interior of the base of the chamber. The cells fit into the hemi-cylindrical wells in the cell mounting post. Sufficient thermal isolation is maintained between the bottom of the cell and the chamber base using teflon TM discs of 1 mm thickness. This is done to insure that the sample-to-bath relaxation time is long in comparison to the period of a.c. temperature response, and yet allow the cells to follow the temperature of the circulating water bath. The cells are held in the wells with an elastic strap. The electrical connections to the heater are routed through small holes drilled in the chamber cap and the electrical connections to the thermisters are routed through holes in the base of the chamber.

The temperature regulated chamber is thermally isolated from the surrounding by a square piece of styrofoam suitably hollowed out to hold the chamber. Figure 12 shows how this assembly is mounted in an aluminum box which also holds the fixed-resistance arms of the wheatstone bridge used to measure the differential a.c. response of the cells. All interconnecting wires in the box are shielded cable (RG-174/U). This provides electrical noise immunity from the heater circuit for the low level a.c. response signal.

All signal connections to the box are made with shielded cable (RG-58/U). Figure 13 shows a schematic representation of these electrical connections to the aluminum box. The sinusoidal signal supplied to the heaters, which are in series to keep any phase difference from being introduced between the two cells, is supplied by a digital frequency synthesizer (Monsanto Model 3100A) at a typical frequency of 0.2 Hz and 5 V amplitude. This signal is also routed to the lock-in amplifier (Ithaco Model 391A) to provide the reference signal it requires. The

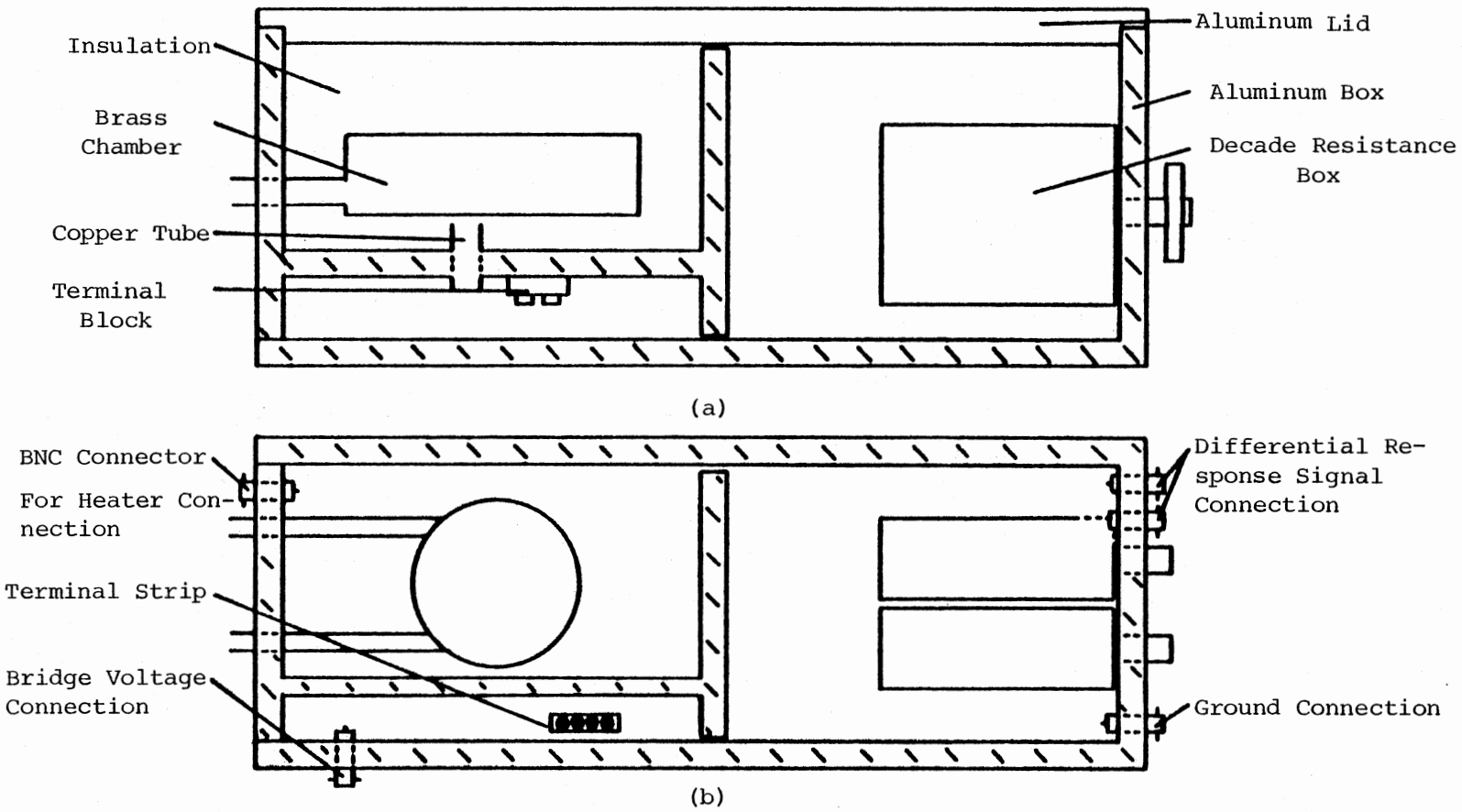

Figure 12. (a) Side View of Aluminum Box That Contains the Sample Cell, Reference Cell, and Wheatstone Bridge Circuit. (b) Top View of Aluminum Box

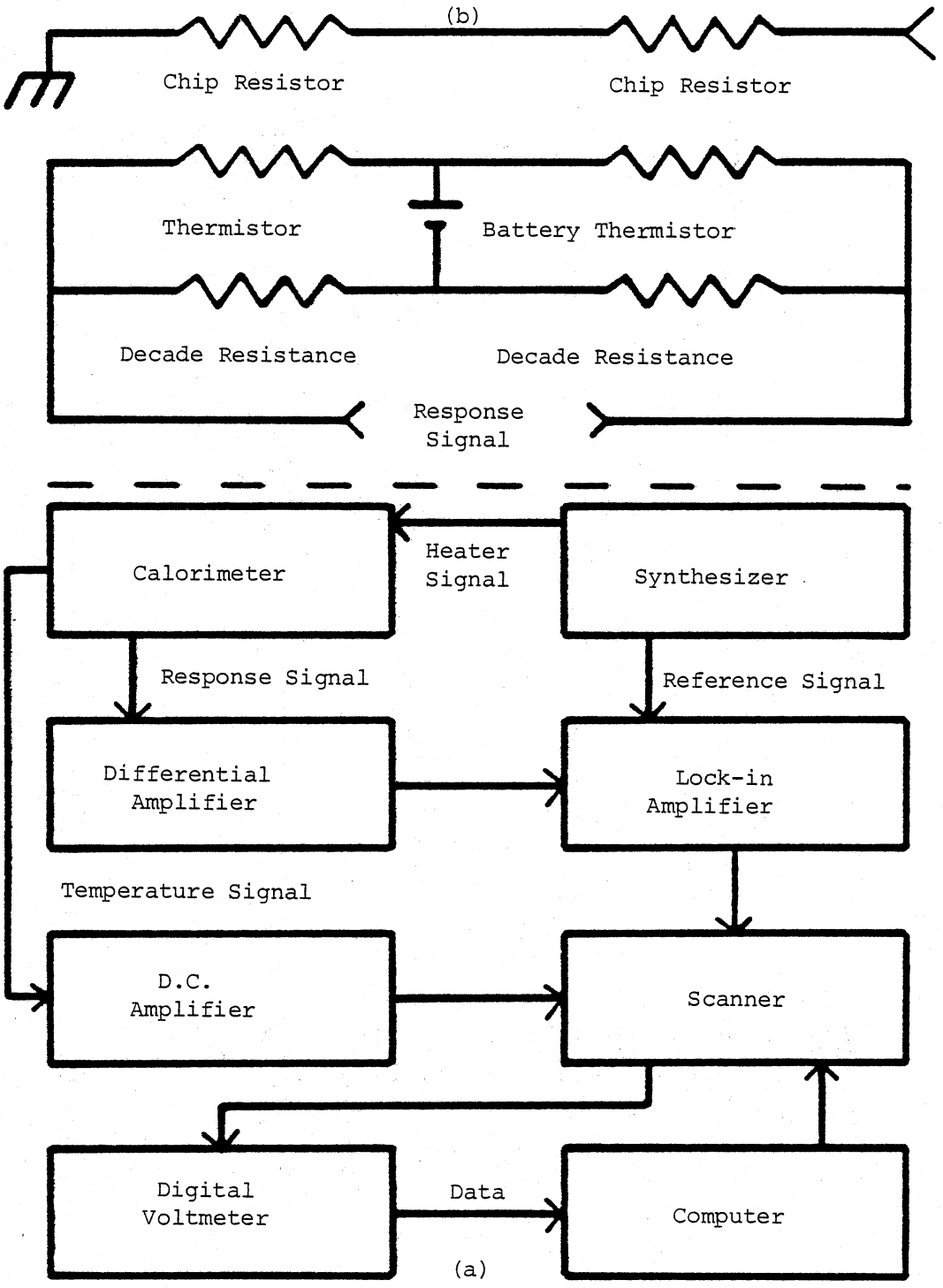

Figure 13. (a) Block Diagram of the Electronics Connected to the Aluminum Box. (b) Schematic Diagram of Electrical Circuits in Aluminum Box

a.c. temperature response signal is routed to the differential amplifier (PAR Model 113), which has an adjustable bandpass. Adjusting the bandpass allows the signal to noise ratio to increase. The lock-in amplifier using this higher level signal outputs a d.c. voltage proportional to the peak amplitude of the differential a.c. response signal by a method known as synchronous detection.

The d.c. mean temperature signal is amplified, by one thousand, by a d.c. nanovolt amplifier (Keithley Model 140) so that it has the same order of magnitude as the a.c. response signal. This allows both values to be read on the 10 V range of the DVM (Keithley Model 5900). These two signals are connected to two of the ten inputs on a scanner (Keithley Model 702). The output of the scanner is connected to the digital voltmeter. This allows a microcomputer (Mits Altair Model 8800A) to control and read the temperature and a.c. response signals. The microcomputer accomplishes this by first directing the scanner to connect the mean temperature signal to the digital voltmeter. The microcomputer then reads this value from the digital voltmeter and stores it in memory. The a.c. response signal is then switched to the digital voltmeter and read in the same manner.

Sample Preparation

DMPC was obtained from CalBioChem and used for sample preparation without further purification. Purified water was obtained by running deionized water, from the available tap in the lab, through an activated charcoal filter to remove any hydrocarbon contaminants, followed by double distillation in a quartz still. The water was stored in quartz flasks. These flasks were periodically cleaned with chromic and phosphoric acid and flushed several times with water from the still before

use. Freshly purified water was used for each sample preparation.

Samples were prepared by placing 10 mg of DMPC in a test tube and adding 0.1 ml of water. This 100 mg DMPC/ml water sample was immersed in a water bath at a temperature of 60 ^{o}C. The sample was removed from the water bath and agitated by hand until the DMPC became suspended. The time required was generally 10-15 s. The sample suspension was re-immersed in the temperature bath until heated. The sample suspension was placed in a vacuum jar and pumped under partial vacuum to remove dissolved gases. This generally required 30-60 s. The sample was cooled immediately in an ice bath and stored overnight at 0^{o}C for use the next day.

Technique

The procedure for loading the cells for an experimental run consisted of 1) flushing both cells with purified water, 2) drying the interior of the cells with a tissue (Kimwipes^{TM}), 3) heating the previously prepared sample to a temperature above the main transition in a water bath, 4) pipeting just enough sample into the sample cell to fill the grooves in the bottom, 5) pipeting sufficient purified water in the reference cell to fill its grooves, 6) installing the top caps on each cell and tightening the cap retaining screws in a manner such that the caps were tightened down evenly. The leads from the heater chips were inserted through the top cap of the brass chamber, and the top cap was lowered into place. As the top cap was lowered into place, care was taken to keep the lead wires from bunching up under the cap. The heater circuit in the box was checked for continuity after soldering the leads to the BNC connection on the aluminum box. This step was necessary as

occasionally the resistor chip-lead wire junction would fail. The top portion of the insulation was placed over the brass chamber, and the aluminum lid was installed on the box and fastened in place with screws.

The system was then cooled from room temperature to a temperature of approximately 10 ^{o}C at a rate of 0.3 ^{o}C/min. The sample was held at 10 ^{o}C for one hour. Most experimental runs were started at a temperature of 20 ^{o}C. So after the one hour period at 10 ^{o}C, the sample was heated to 20 ^{o}C at a rate of 0.3 ^{o}C/min.

The heating signal was set at a frequency of 0.2 Hz with an amplitude of approximately 5 V into the 200 Ω load. The differential amplifier was adjusted so as to have a gain of 1000-2000 and a bandpass from 0.1 to 3 Hz. The reference cell was connected so that only its response signal was measured. The lock-in was adjusted for a sensitivity of 30 mV, and the phase control varied to give a maximum reading of the a.c. response of the reference cell with the time constant set at a value of 40 s. Ten values for the a.c. response of the reference cell were taken by the computer for later use in evaluating the data. The system was then reconnected in the differential mode with the lock-in changed to a sensitivity of 1 mV, and the output zero control varied to bring the reading on scale. This was required because the a.c. response signal from each cell had slightly different phases and amplitudes, and therefore the differential signal was not zero at temperatures far away from the phase transition temperature of the DMPC. The circulator bath was then adjusted to allow the temperature to change by approximately 3^{o}C/hr, while the computer took data points. Every 250 data points were stored on magnetic tape. The program for this is detailed in Appendix A. Data were taken during heating scans, cooling scans and at constant tempera-

ture as detailed in experimental results. The data were analyzed by a computer program which is shown and explained in Appendix B.

CHAPTER IV

EXPERIMENTAL RESULTS

Analysis

As the calorimeter can be operated in the heating or cooling mode, a study was initiated to determine if the main phase transition of DMPC is truly a first order one. This is determined to be true if the transition exhibits hysteresis. A typical result is shown in Figure 14 for 7.7 μℓ of 100 mg/ml suspension, scanned from 20 to 27.6°C at a rate of 1 mdeg/s. The figure shows that on heating the transition peak is a sharp, slightly assymetric one with a half-width ($\Delta T_{\frac{1}{2}}$) of 0.17°C, occurring at 24.00°C. The enthalpy of transition was calculated to be 5.0 kcal/mole. These findings are in excellent agreement with previous results obtained using differential scanning calorimetry (7,8,9). The sample was immediately cooled, upon reaching the maximum temperature, at the same rate as used on heating. One can see that the peak produced is much different than the heating peak. The transition temperature occurred at 23.78°C, thus showing the transition to be first order. Additionally, the peak was much broader, $\Delta T_{\frac{1}{2}}$ = 0.26°C, and reduced in height. The apparent enthalpy change was only 62% of the apparent enthalpy change observed for the heating scan. Thus the thermodynamic path followed by DMPC on the cooling scan was much different than the path followed on the heating scan.

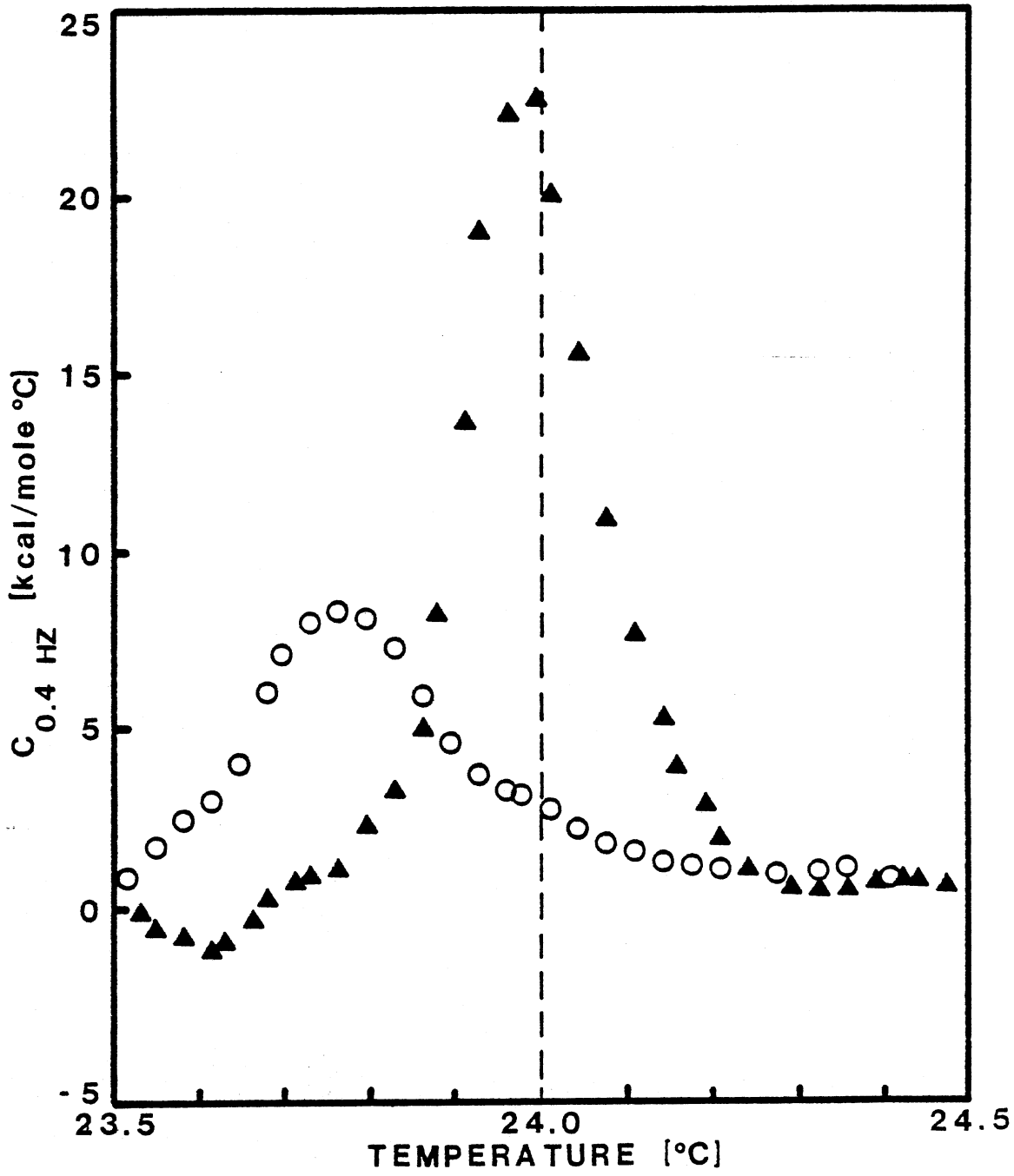

Figure 14. Excess 0.4 Hz A.C. Heat Capacity of DMPC Liposomes Heated (▲) and Cooled (O)

To learn more about this difference in phase transition behavior an annealing study was instigated. Figures 15 and 16, Figures 17 and 18, and Figure 19 show results obtained on three different sample preparations. The average heating transition temperature was 23.98 ± 0.10°C. The difference in values obtained on the same sample was as small as 0.01°C, and no larger than 0.09°C. The average cooling transition temperature was 23.84 + 0.17 - 0.09°C, with differences on the same sample being no greater than 0.08°C. In all cases the cooling transition peak occurred at a temperature less than the heating transition peak. The hysteresis observed was as large as 0.18°C. Both the heating and cooling transition temperatures exhibited no dependence on the previous thermal history of the sample. The peak height variations from sample to sample existed for two reasons. The exact concentration varied from sample to sample, and the concentration of the portions of the sample used could be different than the complete sample preparation. With the small volume of sample prepared a small error in water volume or DMPC mass would lead to a rather large change in concentration. The amount of water evaporated during the degassing process would vary from sample to sample and be unknown. Secondly, the volume of sample contained in the sample cell varied slightly. The top cap was constructed with an outside diameter slightly smaller than the inside diameter of the cell body. This allowed air to escape as the cap was lowered into position. But any excess sample suspension was also forced into the small space between the cap and the cell body. The amount doing so was easily variable and unknown. The variance peak heights on the same sample will be discussed later.

Figures 15 and 16 show the results for a sample that was annealed at 10°C for an hour between successive heating and cooling scans. The heating scans were terminated at temperatures both greater than and less

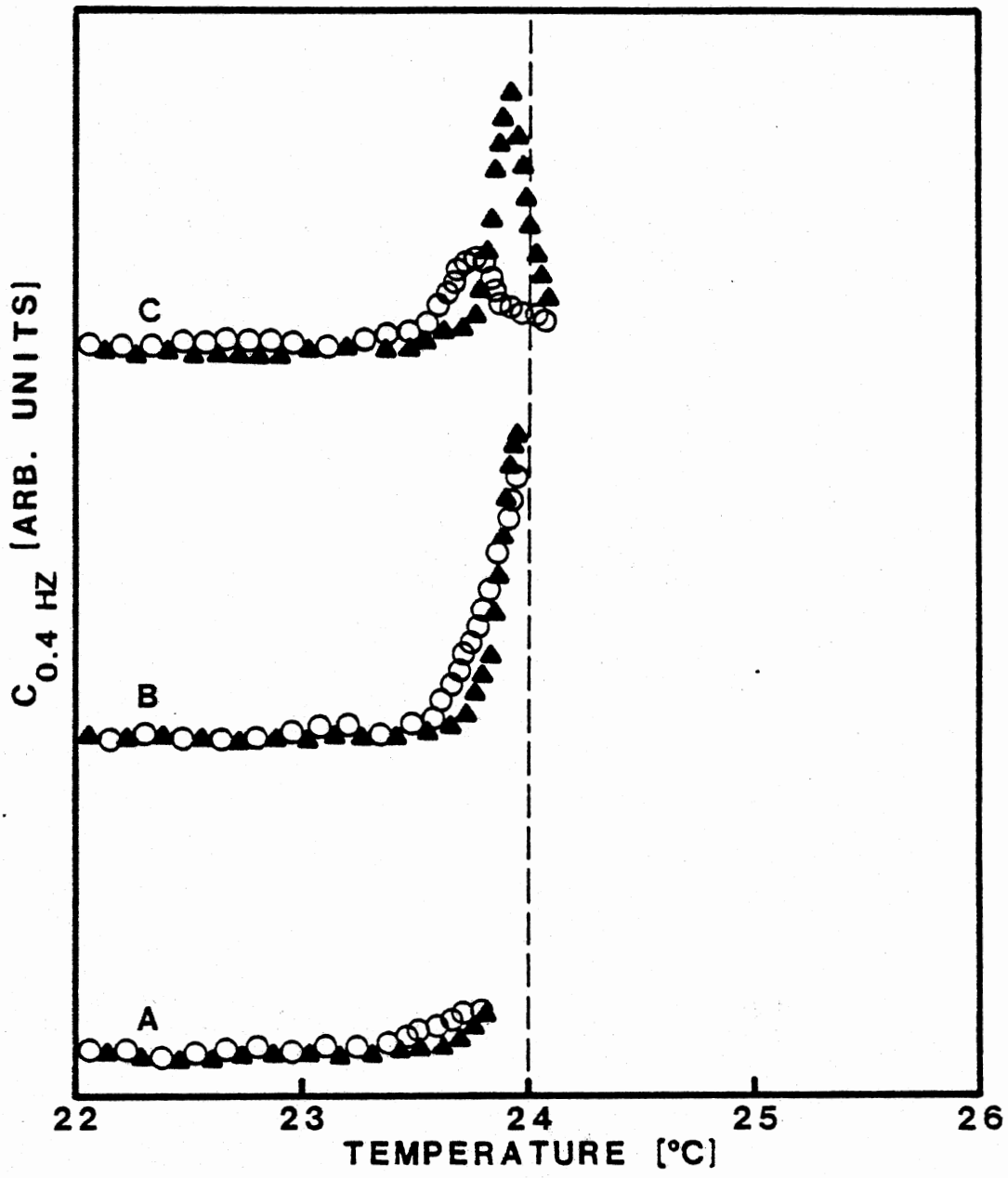

Figure 15. Excess 0.4 Hz A.C. Heat Capacity of DMPC Liposomes (Part 1) Annealed at 10°C for 1 Hr, Heated (▲) to a Maximum Temperature in or Above the Transition Region and Immediately Cooled (O)

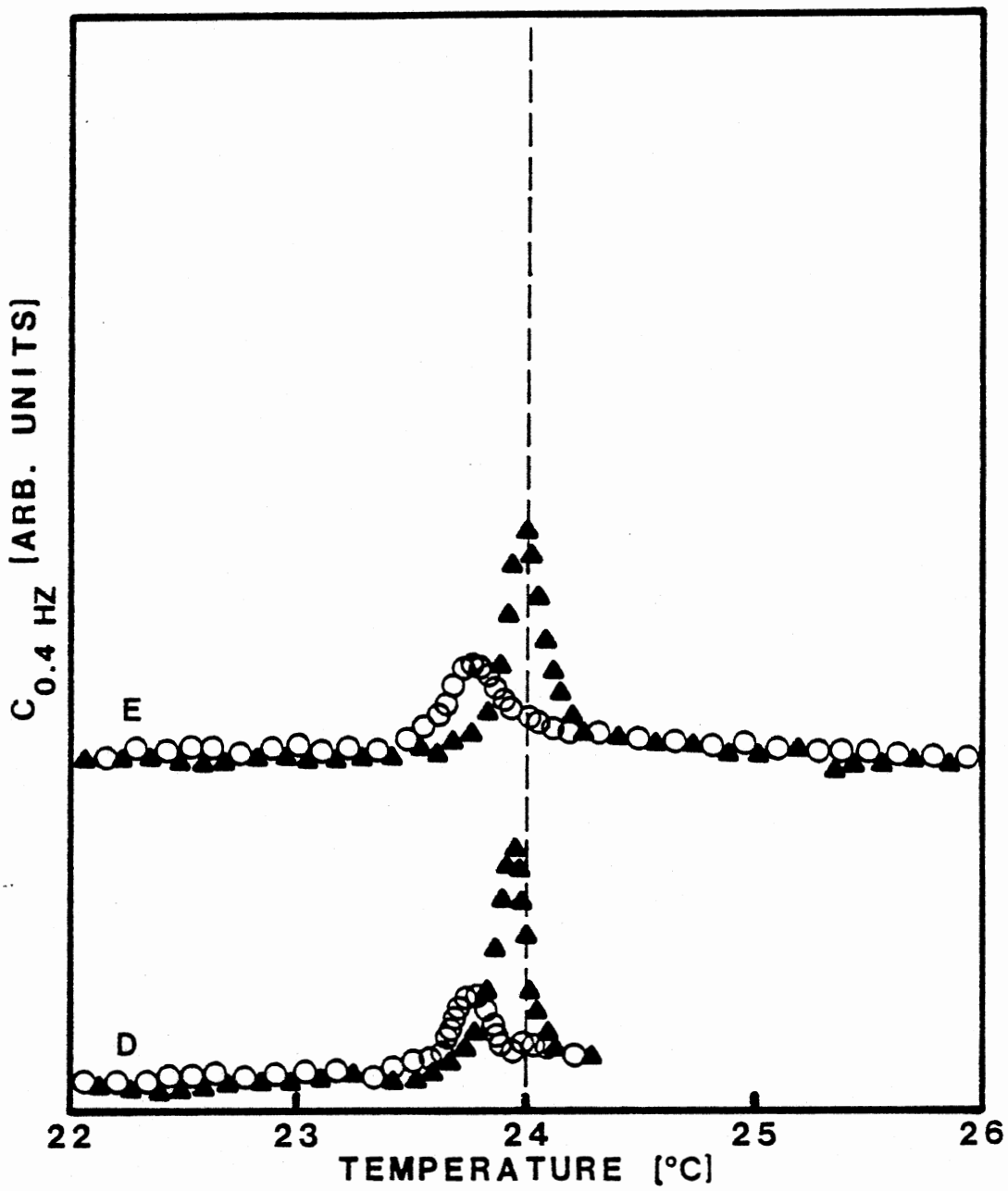

Figure 16. Excess 0.4 Hz A.C. Heat Capacity of DMPC Liposomes (Part 2) Annealed at 10°C for 1 Hr, Heated (▲) to a Maximum Temperature in or Above the Transition Region and Immediately Cooled (O). Run E Annealed at 10°C for 3 Hrs Before Heated and Immediately Cooled

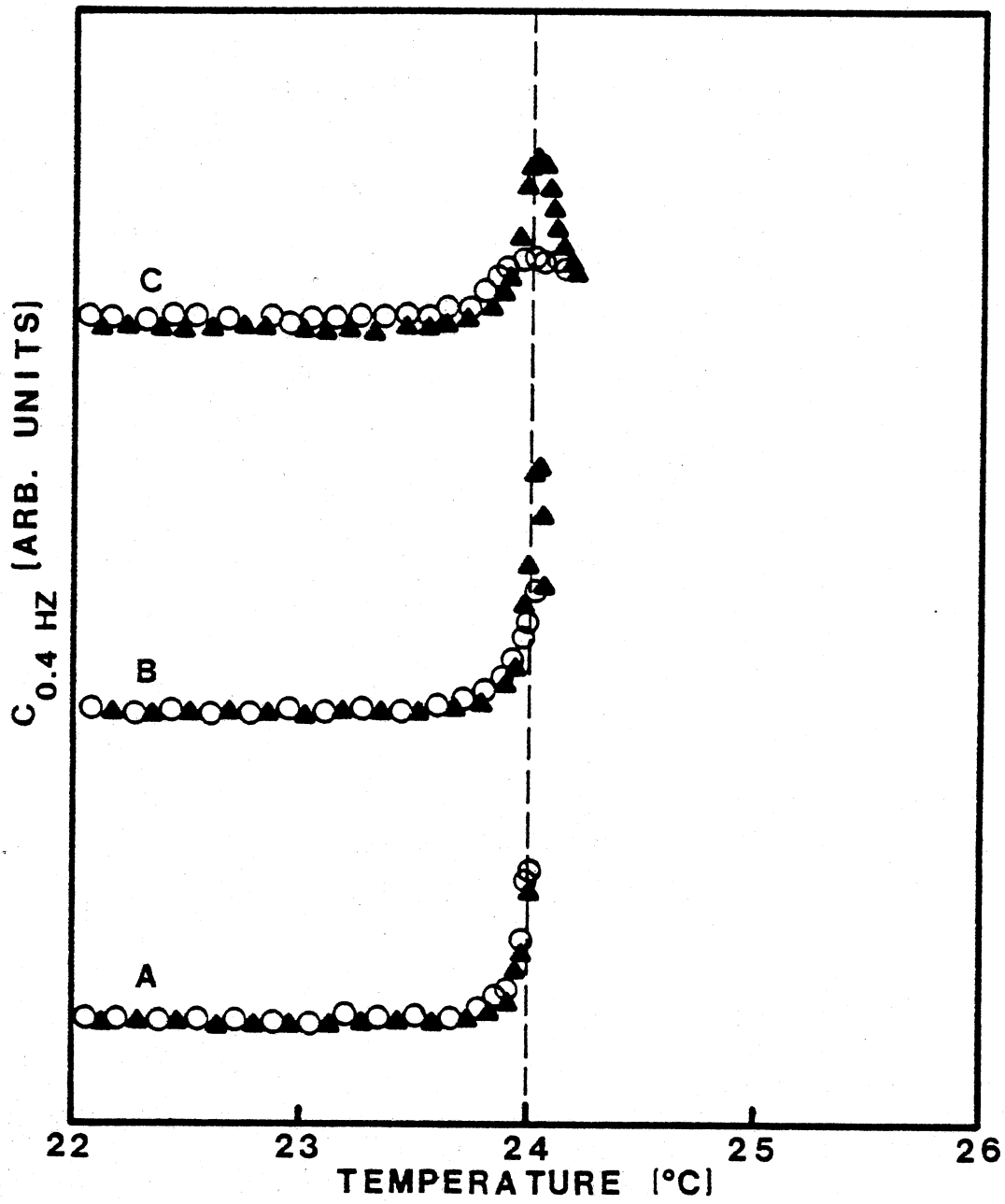

Figure 17. Excess 0.4 Hz A.C. Heat Capacity of DMPC Liposomes (Part 1). Runs A, B, C, Annealed at 10°C for 1 Hr, Heated (▲) to the Maximum Temperature, Held at the Maximum Temperature for 20 Min, Then Cooled (O)

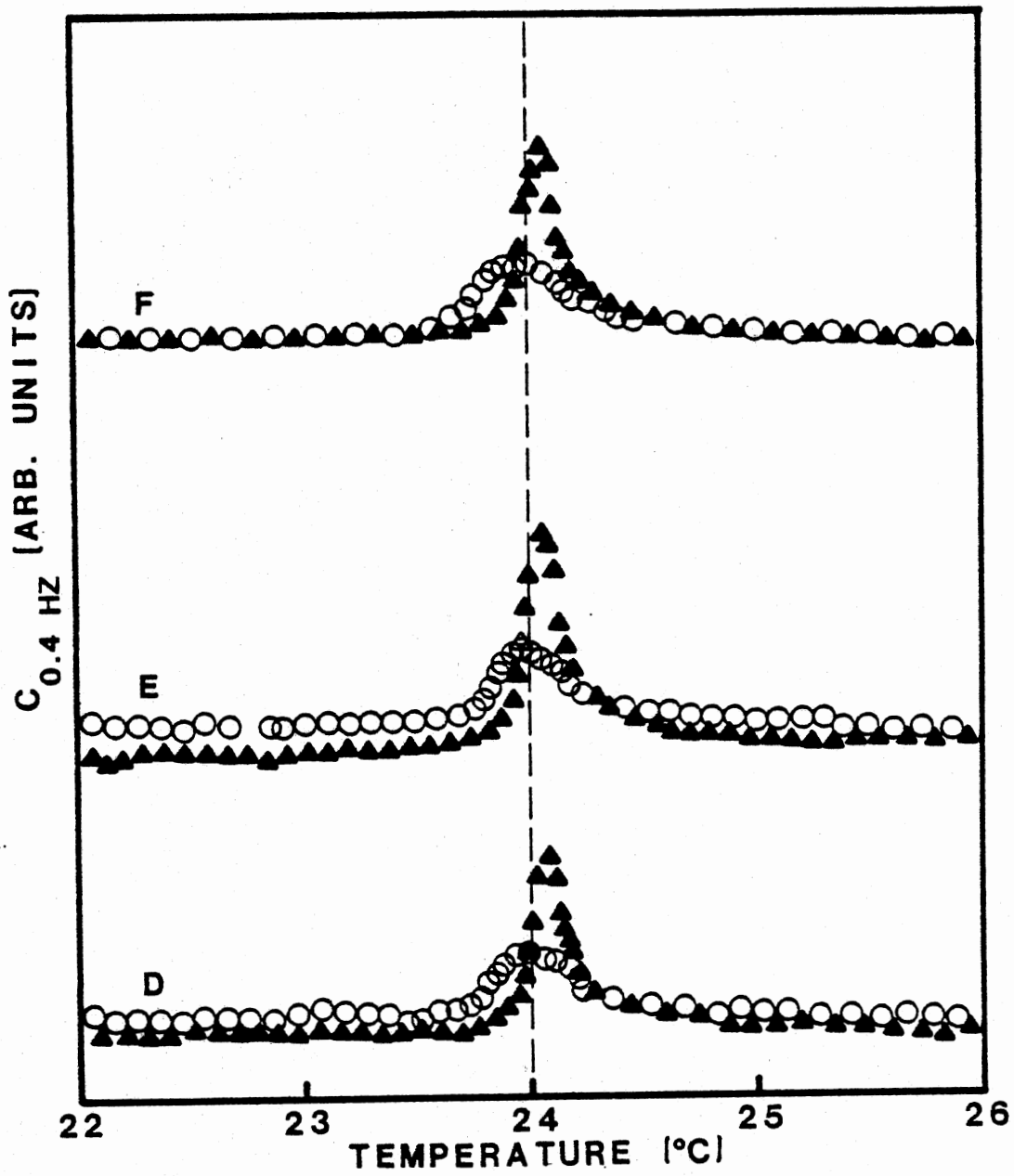

Figure 18. Excess 0.4 Hz A.C. Heat Capacity of DMPC Liposomes (Part 2). Run D Heated (▲) and Immediately Cooled (O). Run E Annealed at 10°C for 16 Hrs Before Heated and Cooled. Run F Annealed at 20°C for 1 Hr Before Heated and Cooled

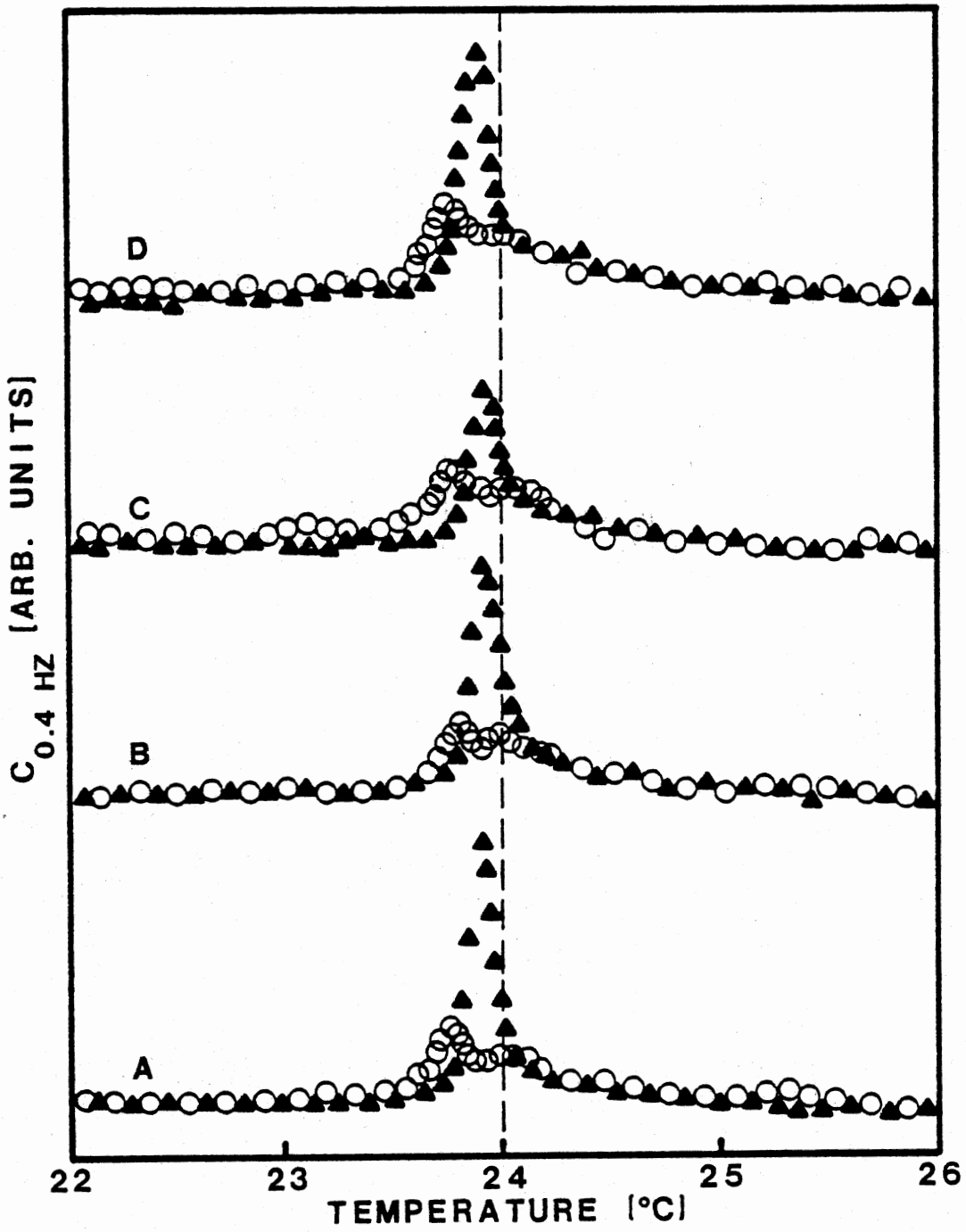

Figure 19. Excess 0.4 Hz A.C. Heat Capacity of DMPC Liposomes. Runs A, B, and D Annealed at 10°C for 1 Hr, Heated (Δ) to 27°C and Immediately Cooled (O). Cooling Run B Annealed at 23.9°C for 20 Min. Run C Annealed at 20°C for 1 Hr, Heated and Immediately Cooled

than the transition temperature. The transition temperature is defined to be the value of the temperature at which the heat capacity of the DMPC reaches its maximum value. All cooling scans began immediately at the termination of the heating scans. All heating scans started at a temperature of 20°C. As the figures show, the cooling scans closely reproduced the heating scans when the heating scans were terminated at a temperature less than the transition temperature. But when the heating scan goes past the transition temperature the heating and cooling peaks become markedly different. The cooling peak for curve E shows only an enthalpy change, between 23 and 25°C, of 1.8 kcal/mole while the heating peak shows an enthalpy change of 4.8 kcal/mole. This value for the heating peak compares favorably to the value found by others. The profiles of the heating peaks remain similar throughout the runs while the cooling peaks do not.

After it was found that the cooling peaks closely reproduced the heating peaks only when the heating scans terminated at a temperature less than the transition temperature, a further study was done to determine the effects of annealing the sample at the maximum temperature reached on a heating scan. The results are found in Figures 17 and 18. The study was done by annealing the sample at the maximum heating scan temperature (± 0.02°C) on runs A, B, and C for 20 min, before starting the cooling scan. This was in addition to the anneal at 10°C for one hour between runs. The heat capacity measured during the 20 min period of constant temperature remained the same. Again the heating and cooling peaks only became noticeably different when the maximum value of the heating scan temperature was greater than the transition temperature. Cooling run B exhibited no peak, as detailed in Figure 20. The

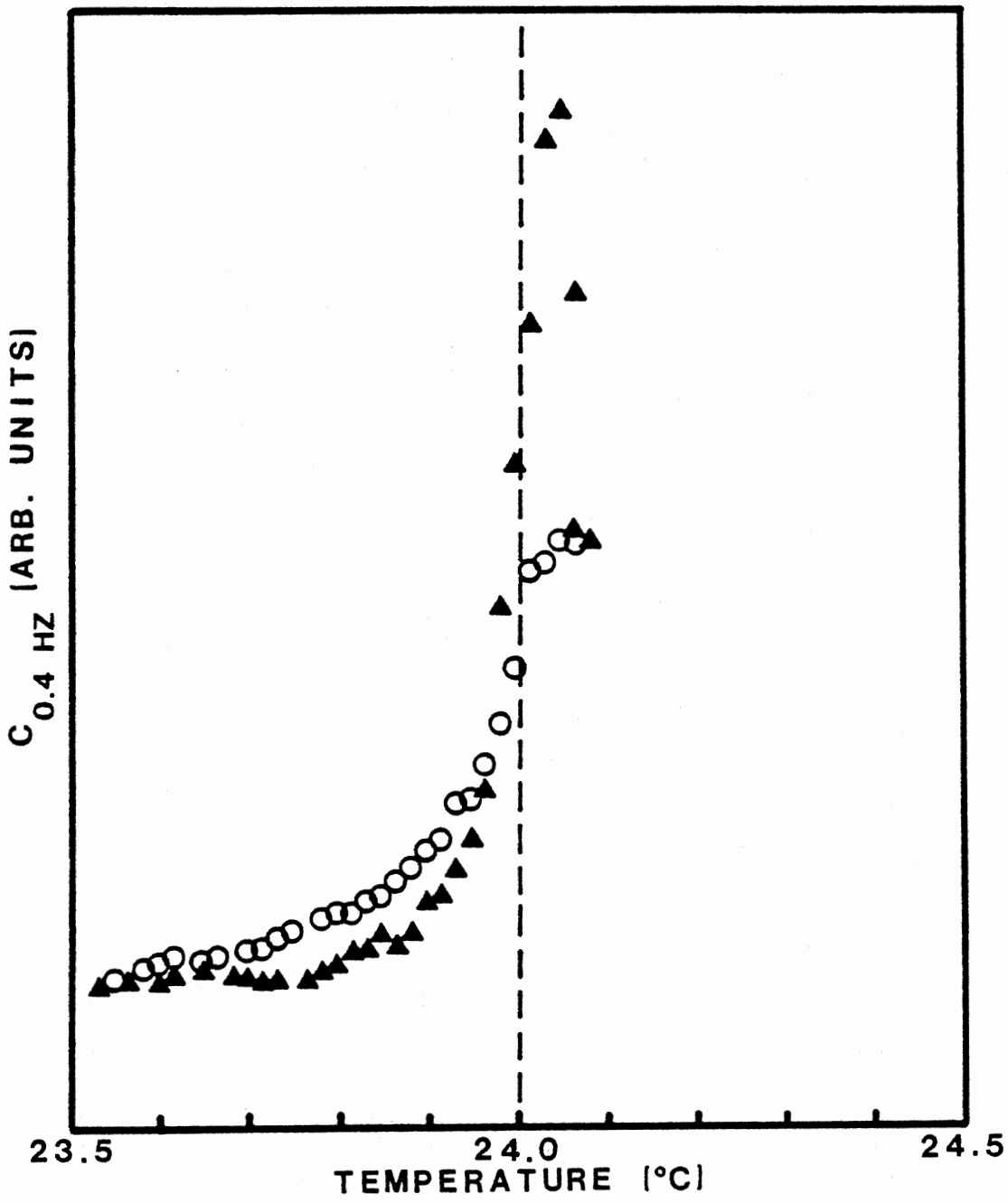

Figure 20. Excess 0.4 Hz A.C. Heat Capacity of DMPC Liposomes. Detail of Figure 17, Run B

heat capacity decreased until it reached a point below the peak observed on heating. At this point the path closely followed the heating scan path. When one compares the peak heights for runs B, the first to reach a temperature greater than the transition temperature (heating), and C one sees that the peak height on heating is greater for run B than for run C. To show that this did not result from the annealing time, heating scan D was taken to a temperature of 27.3°C and immediately cooled. The result shows runs C and D to be similar. Figure 15 also shows this initially larger peak height on heating.

To determine that this reduction in peak height was a result of the previous thermal history of the sample and not a deterioration of the sample, run E was made after a 16 hr anneal at 10°C. As can be seen in the figure the peak height recovered to about two-thirds of its initial height, and upon reheating, run F, the peak height was greater than runs C and D. So the resulting peak heights were due to the previous thermal history of the sample.

Three successive heating scans, all starting at a temperature of 20°C and shown in Figure 21, are the initial scan, a scan after an one hour anneal at 10°C, and a scan after a one hour anneal at 20°C. The figure shows that the scan after an anneal at 10°C produced a peak height reduced by 15% from the initial scan and the peak height is reduced by 43% from the initial scan following the anneal at 20°C. This anneal at 20°C was in the intermediate phase between the pretransition and the main transition.

The complete set of scans is shown in Figure 19. Cooling scan B was held at a temperature of 23.90 ± 0.02°C for 20 min. This temperature corresponds to the transition temperature observed during the heating

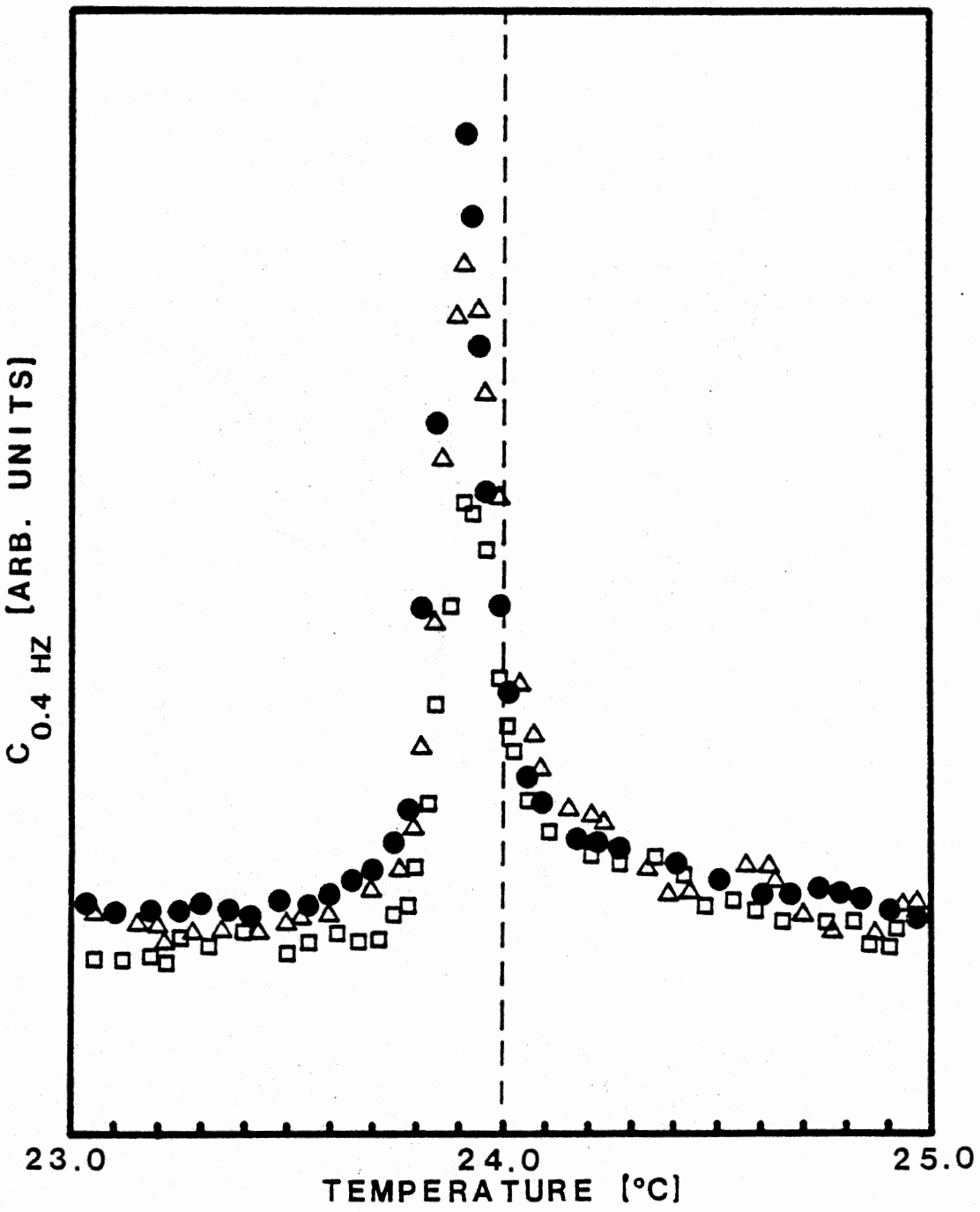

Figure 21. Comparison of Excess 0.4 Hz A.C. Heat Capacity for Heating Scans of DMPC Liposomes Initially Scanned (●), Annealed at 10°C for 1 Hr (Δ), and Annealed at 20°C for 1 Hr (□)

run. The heat capacity did not show any recovery to the value observed on the heating scan, but remained constant. Thus the states the system attains are different and remain so for a considerable amount of time.

Discussion

Others have studied the kinetics of the main transition of DMPC vesicles by temperature jump methods and have found relaxation times of a few milliseconds to a few seconds (41,42). So the differences between the main transition, for heating and cooling scans, found in this work were unexpected. The metastable state indicates that there are relaxation times associated with freezing of the chains that are much longer than a few seconds. The ability of the system to remain in a metastable state for a considerable amount of time would seem to contradict the results of the temperature jump experiments. Thus the a.c. calorimetry technique may be sampling the state of molecular aggregation on a quite different scale than the temperature jump method.

To describe the state of the system more carefully, one should consider the complex liposomal DMPC system as having many different internal degrees of freedom. Each of these degrees of freedom could have its distinct relaxation time, τ_i. If $\tau_i \gg 1/\omega$ where ω is the probe frequency, the particular degree of freedom, i, is not affected by the probe. In this case the effective heat capacity is $C_e = C_{dc} - C_i$, where C_{dc} is the d.c. heat capacity or the total heat capacity due to all degrees of freedom and C_i is the heat capacity due to the unprobed degree of freedom. The relaxation time for the pretransition is known to be one the order of minutes and it is for this reason that the 0.4 Hz a.c. calorimetry used in the work does not detect the pretransition (7). The calorimeter was

sufficiently sensitive to detect the pretransition had it a short enough relaxation time.

The enthalpy of the main transition for a heating scan as measured by the experiment was in good agreement with values measured by differential scanning calorimetry experiments. So the relaxation time for DMPC must be less than the 2.5 s period of the temperature wave. This is in agreement with the temperature jump experiments (41,42).

But the behavior during a cooling scan is quite different. A smaller peak occurs during a cooling scan, which indicates that some degrees of freedom do have a relaxation time of greater than 2.5 sec. As indicated in the data this reduced heat capacity did exist for 20 min. So the relaxation time for some degrees of freedom must be on the order of hours at a temperature of $24^{\circ}C$. Some of these long relaxation times must remain in the ordered phase as the heat capacity does not fully recover its peak value on subsequent reheating after one hour at $10^{\circ}C$.

The results are consistent with the state of molecular organization being quite different for a sample that has been held at a temperature well below the phase transition and one in which the hydrocarbon chains have just frozen. It is possible that the ordering process occurs by the formation of a large number of nucleation sites. These nucleation sites could create a large number of small domains. The time required for these domains to form a cooperative unit whose size is comparable to the well annealed sample could be quite large.

The number of molecules in a cooperative unit can be estimated by a two state van't Hoff analysis of the heat capacity close to the transition. The two state van't Hoff equation can be written as

$$\left(\frac{\partial}{\partial T}\right)_P \ln\left[\frac{\alpha}{1-\alpha}\right] = \frac{\Delta H_{vH}}{RT^2} \tag{6}$$

where α is the fraction of suspension converted from one state to the other, R is the gas constant, and ΔH_{vH} is the standard enthalpy change (43). Taking the derivative and reordering results in

$$\frac{\partial \alpha}{\partial T} = \alpha(1-\alpha)\frac{\Delta H_{vH}}{RT^2} \propto C_{ex} \tag{7}$$

where C_{ex} is the experimentally observed specific heat of the sample. It can be reasonably assumed that at the maximum value of specific heat C_{ex}^{max} the fraction converted is 0.5 at $T = T_m$, where T_m is the temperature value at which C_{ex}^{max} occurs. Taking the ratio of C_{ex}/C_{ex}^{max} gives

$$\frac{C_{ex}}{C_{ex}^{max}} = 4\alpha(1-\alpha)\frac{T_m^2}{T^2} \tag{8}$$

When C_{ex} is equal to 1/2 C_{ex}^{max}, Equation (8) has a value of 0.5. At this point T is approximately equal to T_m for a specific heat peak with small width. The equation has solutions for α that equal 0.147 and 0.853. Integrating Equation (7) and using the values of α determined gives

$$\Delta H_{vH} = \frac{6.98\ T_m^2}{\Delta T_{1/2}} \tag{9}$$

where $\Delta T_{1/2}$ is the width of the peak at half maximum. Equation (9) gives the standard enthalpy change with values that are easily found experimentally. With the approximations used the accuracy is within 10%. The size of a cooperative unit is determined by the ratio $\frac{\Delta H_{vH}}{\Delta H_{cal}}$ where ΔH_{cal}

is the enthalpy change measured experimentally.

This representation by a two state system is an over simplification, but does give an order of magnitude estimate of the size of the cooperative unit and a comparison of the size between a well ordered sample and one just reordered. The analysis of the heating peak gives a value of 600-800 molecules/cooperative unit. The same analysis for the cooling peak gives a size of 200-450 molecules/cooperative unit. This could only be an average size for the cooperative unit and values larger and smaller are to be expected.

The cooperative unit is identified as a domain in the lipid bilayer. The fractional number of lipid molecules on the domain boundary varies from 25-30% for a 200 molecule cooperative unit to 10% for a 800 molecule cooperative unit, as determined by considering a one-molecule-wide ring on the circumference of a circular domain. So from these numbers one sees that a considerable fraction of the molecules in a domain lie on the domain boundary. Immediately after the reordering process starts these domains most probably would have different molecular orientations. The process of reorientation of many molecules to form larger domains would require a considerable amount of time. The heat capacity would then not recover until the boundary lipids had accomplished this reorientation to the ordered state.

As seen in the discussion, calorimetry is sensitive to the long range order in the bilayer. Molecular probes used in spin resonance and fluorescence studies tend to sample the local environment and even contribute nucleation sites upon which the reordering process starts. These probes then tend to be in the region where most rapid reordering occurs. Thus, they preferentially measure the rapid short range ordering

process and are relatively insensitive to the slow process of long range ordering.

These domains within the bilayer have been experimentally observed with wet-stage electron microscopy (44). Additionally the ordered and disordered phases have been observed, by deuterium NMR studies, to coexist in samples of DPPC when cooled below the transition temperature (30). This coexistence of phases has been observed to exist for a time of at least 30 min and shows that the relaxation time is large as this calorimetric study infers.

Summary and Conclusions

The heat capacity of 100 mg of DMPC/ml of water was measured during heating scans and cooling scans with various anneal temperatures and anneal times both above and below the main transition. The results showed that the cooling scan heat capacity peaks closely resembled the peaks obtained during a heating scan only when the maximum temperature reached during the heating scan was less than the transition temperature. When a sample was scanned through a temperature greater than the transition temperature and then subsequently cooled down through the transition, a specific heat peak was produced that was shifted downward in temperature, broadened, and reduced in height. The apparent enthalpy change was only approximately 60% of the apparent enthalpy change measured for a peak obtained on a heating scan. A sample held at a constant temperature, within the width of the transition, showed no tendency to recover the peak height for periods as long as 20 min. Subsequent reheating scans produced a peak height smaller than that produced during the first heating scan. The amount of the peak

height recovered depended on the length of time the sample was annealed at 10°C. A larger amount of time produced a greater peak height recovery.

The hysteresis in the transition temperature demonstrated conclusively that the transition is a first order one. The significantly different peaks observed indicates that DMPC follows a different thermodynamic path on a cooling scan, when scanned from a temperature greater than the heating transition temperature, than it does on a heating scan. This metastable state exists for periods of at least 20 min at the transition temperature and as indicated by the small reduction in peak height for subsequent heating scans may be hours.

BIBLIOGRAPHY

1. Dyson, R. D., Essentials of Cell Biology (Allyn and Bacon, Inc., Boston, 1978).

2. De Robertis, E. D. P., W. W. Nowinski, and F. A. Saez, Cell Biology (W. B. Saunders Co., Philadelphia, 1965).

3. Danielli, J. F., in Cell Membranes, eds. G. Weissmann and R. Claiborne, p. 3 (H. P. Publishing Co., Inc., New York, 1975).

4. Nagle, J. F. and H. L. Scott, Physics Today 31, 38 (1978).

5. Melchior, D. L. and J. M. Steim, Annu. Rev. Biophys. Bioeng. 5, 205 (1976).

6. Mabrey, S. and J. M. Sturtevant, Proc. Natl. Acad. Sci. (USA) 73, 3862 (1976).

7. Lentz, B. R., E. Freire, and R. L. Biltonen, Biochemistry 17, 4475 (1978).

8. Mountcastle, D. B., R. L. Biltonen and M. J. Halsey, Proc. Natl. Acad. Sci. (USA) 75, 4906 (1978).

9. Mabrey, S. and J. M. Sturtevant, Biochem. Biophys. Acta 486, 444 (1977).

10. Melchoir, D. L., H. J. Morowitz, J. M. Sturtevant, and T. Y. Tsong, Biochem. Biophys. Acta 219, 114 (1970).

11. Nichols, P. and N. Miller, Biochem. Biophys. Acta 356, 184 (1974).

12. Blok, M. C., L. L. M. Van Deenen, and J. De Gier, Biochem. Biophys. Acta 433, 1 (1976).

13. Inove, K., Biochem. Biophys. Acta 339, 390 (1974).

14. Papahadjopoulos, D., K. Jacobson, S. Nir and T. Isac, Biochem. Biophys. Acta 311, 330 (1973).

15. Blok, M. C., E. C. M. Van Der Neut-Kok, L. L. M. Van Deenen, and J. De Gier, Biochem. Biophys. Acta 406, 187 (1975).

16. Esfahani, M., A. R. Limbrick, S. Knotton, T. Oka, and S. J. Waki, Proc. Natl. Acad. Sci. (USA) 68, 3180 (1971).

17. Ovarth, P., H. V. Schairer and W. Stoffel, Proc. Natl. Acad. Sci. (USA) 67, 606 (1970).

18. Raison, J. K., J. M. Lyons, R. J. Mehlhorn and A. D. Keith, J. Biol. Chem. 246, 4036 (1971).

19. Deamer, D. and A. D. Bangham, Biochem. Biophys. Acta 443, 629 (1976).

20. Papahadjopoulos, D., W. J. Vail, K. Jacobson and G. Poste, Biochem. Biophys. Acta 394, 483 (1975).

21. Luzzati, V., Biol. Memb. 1, 71 (1968).

22. Tardieu, A. and V. Luzzati, J. Mol. Biol. 75, 711 (1973).

23. Laggner, P., A. M. Gotto, Jr. and J. D. Morrisetti, Biochemistry 18, 164 (1979).

24. Luzzati, V. and A. Tardieu, Annu. Rev. Phys.Chem. 25, 79 (1974).

25. Janiak, M. J., D. M. Small and G. G. Shipley, Biochemistry 15, 4575 (1976).

26. Janiak, M. J., D. M. Small and G. G. Shipley, J. Biol. Chem. 254, 6068 (1979).

27. Chen, S. C., J. M. Sturtevant and B. J. Gaffney, Proc. Natl. Acad. Sci. (USA) 77, 5060 (1980).

28. Füldner, H. H., Biochemistry 20, 5707 (1981).

29. Gaber, B. P., P. Yager and W. L. Peticolas, Biophys. J. 24, 677 (1978).

30. Davis, J. M., Biophys. J. 27 339 (1979).

31. Seelig, J. and W. Niederberger, Biochemistry 13, 4839 (1974).

32. Seelig, A. and J. Seelig, Biochem. Biophys. Acta 406, 1 (1975).

33. Roberts, M. F., A. A. Bothner-By and E. A. Dennis, Biochemistry 17, 935 (1978).

34. Griffin, R. G., L. Powers and P. S. Pershan, Biochemistry 17, 2718 (1978).

35. Nagle, J. F., Annu. Rev. Phys. Chem. 31, 157 (1980).

36. Marcelja, S., Biochem. Biophys. Acta 367, 165 (1974).

37. Belle, J. and P. Bothorel, Nouv. Jour. Chim. 1, 265 (1977).

38. Scott, H. L. and W. Cheng, Biophys. J. 28, 117 (1979).

39. Sullivan, P. F. and G. Seidel, Phys. Rev. 173, 679 (1968).

40. Schwartz, P., Phys. Rev. B 4, 920 (1971).

41. Tsong, T. Y., Proc. Natl. Acad. Sci. (USA) 71, 2684 (1974).

42. Tsong, T. Y. and M. I. Kanehisa, Biochemistry 16, 2674 (1977).

43. Mabrey, S. and J. M. Sturtevant, in Methods in Membrane Biology, ed. E. D. Korn, 9, p. 237 (Plenum Press, New York, 1978).

44. Hui, S. W. and D. F. Parsons, Science 190, 383 (1975).

45. Temperature Measurement Handbook, p. A-11 (Omega Engineering, Inc., Stamford, Connecticut, 1980).

APPENDIX A

COMPUTER PROGRAM THAT READS THE DATA

```
10 DIM DA(2,500)
20 REM COMPUTER COMMANDS DMM TO MAKE MEASUREMENT
30 REM THEN WHEN DATA IS READY IT IS READ
40 MJ=1
50 PRINT "THE COMPUTER WILL READ THE AC TEMPERATURE, TAC, AND"
60 PRINT "THE MEAN TEMPERATURE OF THE SAMPLE CELL, T"
70 PRINT
80 JJ=1
90 INPUT "THE TWO CHANNELS TO BE READ, TAC FIRST";C1,C2
100 INPUT "THE INTERVAL BETWEEN DATA SETS IN MACHINE CYCLES"; IT
110 OUT 36,0
120 OUT 38,0
130 OUT 37,0
140 OUT 39,111
150 OUT 36,4
160 OUT 38,4
170 OUT 39,255
180 OUT 32,0
190 OUT 34,0
200 OUT 33,0
210 OUT 35,0
220 OUT 32,4
230 OUT 34,4
240 S=O
250 X=1/10
260 Y=1/100
270 Z=1/1000
280 Z1=1/10000
290 Z2=Z1/10
300 CH=C1
310 CK=CH+240
320 OUT 39,CK
330 FOR J=1 TO 110
340 NEXT J
350 OUT 39,CH
360 OUT 39,CK
370 STAT=INP(39)
380 IF STAT>=128 THEN GOTO 370
390 LET A=INP(33)
400 LET B=INP(35)
410 LET G=INP(37)
420 C=INT(A/16)
430 IF A>15 THEN D-A=16
440 IF A<15 THEN D=A
450 E=INT(B/16)
460 IF B>9 THEN F=B-E*16
470 IF B<=9 THEN F=B
480 H=INT(G/16)
490 IF G>9 THEN I=G-H*16
500 IF G<=9 THEN I=G
510 S=C+D*X+E*Y+F*Z+H*Z1+I*Z2
520 STAT =STAT-CH
530 IF STAT >=111 THEN S=-S
540 DA(1,JJ)=CH
```

```
550 DA(2,JJ)=S
560 PRINT JJ,CH,S
570 JJ=JJ+1
580 IF JJ>500 THEN 650
590 IF CH=C1 THEN CH=C2 ELSE CH=C1
600 IF CH =C2 THEN 310
610 FOR J=1 TO IT
620 NEXT
630 PRINT
640 GOTO 310
650 ON MJ GOTO 690, 710,730,750,770,790,810,830,850,870,890,910,930
660 PRINT "OUT OF ARRAYS FOR TAPE STORAGE"
670 PRINT ""
680 GOTO 660
690 CSAVE "*DA DA1 :O
700 GOTO 940
710 CSAVE "*DA DA2 :O
720 GOTO 940
730 CSAVE "*DA DA3 :O
740 GOTO 940
750 CSAVE "*DA DA4 :O
760 GOTO 940
770 CSAVE "*DA DA5 :O
780 GOTO 940
790 CSAVE "*DA DA6 :O
800 GOTO 940
810 CSAVE "*DA DA7 :O
820 GOTO 940
830 CSAVE "*DA DA8 :O
840 GOTO 940
850 CSAVE "*DA DA9 :O
860 GOTO 940
870 CSAVE "*DA DA10 :O
880 GOTO 940
890 CSAVE "*DA DA11 :O
900 GOTO 940
910 CSAVE "*DA DA12 :O
920 GOTO 940
930 CSAVE "*DA DA13 :O
940 MJ=MJ+1
950 JJ=1
960 CH=C1
970 GOTO 310
```

APPENDIX B

COMPUTER PROGRAM THAT ANALYZES THE DATA AND EXPLANATION OF THE PROGRAM

```
10 INPUT "NUMBER OF DATA FILES";FE
20 P=1
30 AC#=O
40 DIM AR(2,500)
50 DIM CC#(1,10)
60 INPUT "RESISTANCE OF BRIDGE ARM IN lOOK";RO
70 INPUT "EMF OF BATTERY";EB
80 INPUT "HEATER PEAK VOLTAGE";EH
90 INPUT "HEATER FREQUENCY";HF
100 INPUT "GAIN OF PREAMP FOR REF CELL";PG
110 RO=RO*100000!
120 HF=HF*6.28319
130 A#=1.2833977D-03
140 B#=2.3635177D-04
150 C#=9.2562822D-08
160 D#=.08617284#
170 E#=.069574531#
180 F#=4.0740741D-04
190 G#=6.1728395D-06
200 INPUT "LOCK-IN SENSITIVITY IN VOLTS FOR REF";G
210 CLOAD "*AR DA1 :O
220 M=2
230 N=1
240 FOR I=1 TO 10
250 GOSUB 930
260 CC#(1,I)=PG*EH*EH*EB*(RO-(2*R#))/(1600*AR(2,N)*G*HF*RO*RO*TR#)
270 PRINT CC#(1,I)
280 M=M+2
290 N=N+2
300 AC#=AC#+CC#(1,I)
310 NEXT I
320 CR#=AC#/10
330 INPUT "GAIN OF PREAMP FOR DIFFERENTIAL";PG
340 INPUT "LOCK-IN SENSITIVITY IN VOLTS FOR DIF";G
350 M=22
360 N=21
370 GOSUB 1120
380 ZZ=FE-1
390 P=1
400 CLOAD "*AR DA2 :O
410 N=1
420 M=2
430 GOSUB 1120
440 ZZ=ZZ-1
450 P=1
460 CLOAD "*AR DA3 :O
470 N=1
480 M=2
490 GOSUB 1120
500 ZZ=ZZ-1
510 P=1
520 CLOAD "*AR DA4 :O
530 N=1
540 M=2
```

```
550 GOSUB 1120
560 ZZ=ZZ-1
570 P=1
580 CLOAD "*AR DA5 :O
590 N=1
600 M=2
610 GOSUB 1120
620 ZZ=ZZ-1
630 P=1
640 CLOAD "*AR DA6 :O
650 N=1
660 M=2
670 GOSUB 1120
680 ZZ=ZZ-1
690 P=1
700 CLOAD "*AR DA7 :O
710 N=1
720 M=2
730 GOSUB 1120
740 ZZ=ZZ-1
750 P=1
760 CLOAD "*AR DA8 :O
770 N=1
780 M=2
790 GOSUB 1120
800 ZZ=ZZ-1
810 P=1
820 CLOAD "*AR DA9 :O
830 N=1
840 M=2
850 GOSUB 1120
860 ZZ=ZZ-1
870 P=1
880 CLOAD "*AR DA10 :O
890 N=1
900 M=2
910 GOSUB 1120
920 ZZ=ZZ-1
930 AR(2,M)=AR(2,M)*100
940 T1#=(AR(2,M)+D#)/E#
950 T#=(AR(2,M)+D#)/E#+((F#/E#)*T1#*T1#)-((G#/E#)*T1#*T1#*T1#)
960 TD#=T1#-T#
970 TD#=ABS(TD#)
980 IF TD#<=1D-04 GOTO 1010
990 T1#=T#
1000 GOTO 950
1010 T=T#+273.18
1020 IT#=1/T
1030 R1#=EXP((IT#-A#)/B#)
1040 R#=EXP((IT#-A#-C#*LOG(R1#)*LOG(R1#)*LOG(R1#))/B#)
1050 RD#=R1#-R#
1060 RD#=ABS(RD#)
1070 IF RD#<=.05 GOTO 1100
```

```
1080 R1#=R#
1090 GOTO 1040
1100 TR#=-T*T*(B#+3*C#*LOG(R#)*LOG(R#))/R#
1110 RETURN
1120 INPUT "LOCK-IN OFFSET AS TIMES FULL SCALE";UO
1130 UO=UO*G
1140 PRINT "N STOP POINT IS THE NEXT N TO COME UP"
1150 INPUT "N STOP POINT";NS
1160 GOSUB 930
1170 Q1#=RO/PG
1180 Q2#=RO-(2*R#)
1190 Q3=AR(2,N)*G
1200 Q4=UO+Q3
1210 Q5=TR#*RO*HF*CR#*CR#
1220 Q6=EB*EH*EH
1230 CS=Q1#*1600*Q5*Q4/(Q2#*Q6)
1240 T=T-273.18
1250 AR(1,P)=-CS
1260 AR(2,P)=T
1270 PRINT "HEAT CAPACITY";CS,"TEMPERATURE";T,"P";P
1280 N=N+2
1290 M=M+2
1300 IF N=501 GOTO 1340
1310 P=P+1
1320 IF N=NS GOTO 1120
1330 GOTO 1160
1340 RETURN
```

The program calculates the heat capacity of the sample using the value of the differential response signal and the value of the response signal from the reference cell. The equation that describes the heat capacity of the reference cell and the sample is derived by using a representation of the circuit as shown in Figure 13, where R is the d.c. resistance value of each thermistor, δR_s and δR_r are the oscillating resistance values for the sample cell and the reference cell thermistors, R_o is the resistance of each decade resistance box, and V_b is the voltage of the battery. The voltage across the sample cell thermistor is

$$V_1 \simeq (V_b/R_o)(R + \delta R_s)\left(1 - \frac{R + \delta R_s}{R_o}\right) \tag{1}$$

for $R << R_o$, and the voltage across the reference cell thermistor is

$$V_2 \simeq (V_b/R_o)(R + \delta R_r)\left(1 - \frac{R + \delta R_r}{R_o}\right) \tag{2}$$

for $R << R_o$. The differential voltage, ΔV, is then

$$\Delta V = V_1 - V_2 = (V_b/R_o^2)\left[(R_o - 2R) - (\delta R_s + \delta R_r)\right](\delta R_s - \delta R_r) \tag{3}$$

after some algebra. For this case $R_o - 2R >> \delta R_3 + \delta R_r$, and thus $\delta R_s + \delta R_r$ can be dropped. The result for the differential voltage is then

$$\Delta V = (V_b/R_o^2)(R_o - 2R)(\delta R_s - \delta R_r) \tag{4}$$

The oscillating values of temperature for the sample and reference cells are related to the oscillating values of the thermistor resistances by

$$\delta R_s = \delta T_s \frac{dR}{dT} \tag{5}$$

and

$$\delta R_r = \delta T_r \frac{dR}{dT} \tag{6}$$

The input power amplitude, $\dot{q}_o$, is calculated from the value of the input voltage to the heaters, $V_h = V_o \sin\omega t$, and the resistance, h, of each heater chip. The result for the input power, $\dot{q}$, to each cell is

$$\dot{q} = \dot{q}_o e^{i2\omega t} = -(V_o^2/8h) e^{i2\omega t} \tag{7}$$

where ω is the frequency of the sinusoid. The differential equation that describes the oscillating value of temperature for each cell is

$$C \frac{\partial T}{\partial t} = \dot{q} - T/R \tag{8}$$

where C is the heat capacity, and R is the thermal resistance between the cell and its surroundings. Equation (8) has the solution

$$T = \delta T e^{i2\omega t} = -i(V_o^2/16h\omega C) e^{i2\omega t} \tag{9}$$

when RC >> 1. Combining Equation (5), (6) and (9) and using the results in Equation (4) gives

$$\Delta V = -(V_b/R_o^2)(R_o - 2R) \frac{dR}{dT} (V_o^2/16h\omega)(1/C_s - 1/C_r) \tag{10}$$

where C_s is the heat capacity of the sample cell and C_r is the heat capacity of the reference cell. The heat capacity of the sample cell is equal to the heat capacity of the sample, C_{sp}, and the heat capacity of the cell. The heat capacity of the cell is the same as the reference cell. Thus the heat capacity of the sample cell is

$$C_s = C_{sp} + C_r \tag{11}$$

With the approximation that $C_{sp} >> C_r$, Equation (10) become

$$C_{sp} = -[R_o^2(16h\omega)\Delta V/C_r^2]/[V_b V_o^2(R_o-2R)\frac{dR}{dT}] \tag{12}$$

The heat capacity of the reference cell is calculated from Equation (2). With the d.c. voltage component dropped, the result is

$$\delta V_2 = (V_b/R_o^2)((R_o-2R)\delta R_r - \delta R_r^2) \tag{13}$$

The solution for the heat capacity of the reference cell is

$$C_r = (V_b V_o^2(R_o-2R)/16R_o^2\, h\omega \frac{dR}{dT})\frac{1}{\delta V_2} \tag{14}$$

with the use of Equations (6) and (9), and δR_r^2 dropped, as $(R_o-2R)\delta R_r$ is $>> \delta R_r^2$.

The mean temperature is calculated from the thermocouple voltage, V_t, using

$$V_t = a + bT = cT^2 + dT^3 \tag{15}$$

where a,b,c, and d are coefficients calculated using known values of V_t and T from a table (45). Once the temperature is known the resistance, R, of a thermocouple can be calculated using

$$1/T = A + B\ \ln(R) + C\ \ln^3(R) \tag{16}$$

where A, B, C are coefficients calculated using known values of R and T from a table (45). The derivative of Equation (16) with respect to T

gives

$$\frac{dR}{dT} = -(R/T^2)(B + 3C \ln^2(R)) \qquad (17)$$

and thus the heat capacity of the sample can be calculated.

VITA

Steven Gayle Black

Candidate for the Degree of

Doctor of Philosophy

Thesis: A.C. CALORIMETRY OF DMPC LIPOSOMES

Major Field: Physics

Biographical:

Personal Data: Born in Iola, Kansas, October 14, 1954, the son of Mr. and Mrs. I. G. Black.

Education: Graduated from Eureka High School, Eureka, Kansas, in May, 1972; received Bachelor of Science degree in physics from Emporia State University in May, 1976; completed requirements for the Doctor of Philosophy degree at Oklahoma State University, Stillwater, Oklahoma, in July, 1982.

Professional Experience: Graduate Teaching Assistant, Oklahoma State University, 1976-1979; Graduate Research Assistant, Oklahoma State University, 1980-1982.